

**AN INVESTIGATION INTO TRANSIENT PRESSURE  
PULSES FOR GAS-SOLIDS FLOW**

**A  
Thesis**

*Submitted in partial fulfillment of the requirement for the award of degree of*

**Master of Engineering  
In  
Thermal Engineering**

*Submitted by*

**AMIT GOEL  
(ROLL NO. 801383002)**



**UNDER THE GUIDANCE OF**

**Dr. S.S. MALLICK**

**Mr. ATUL SHARMA**

**(ASSISTANT PROFESSOR)**

**(LECTURER)**

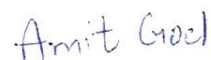
**DEPARTMENT OF MECHANICAL ENGINEERING  
THAPAR UNIVERSITY, PATIALA – 147004  
JULY 2015**

## CERTIFICATION

I, **Amit Goel**, declare that this thesis report entitled “*An Investigation into Transient Pressure Pulses for Gas-Solids Flow*”, submitted towards fulfillment of the requirements for the award of Master’s Degree in Thermal Engineering, in Mechanical Engineering Department of Thapar University, Patiala, is entirely my own work. This document has not been submitted for any degree in any other institution.

Date: 13/07/2015

Place: Patiala



**Amit Goel**

801383002

Thapar University, Patiala

This is to certify that above statement made by the candidate is correct and true to the best of my knowledge.



**Dr. S.S. Mallick**

(Assistant Professor)

Mechanical Engineering Department

Thapar University, Patiala



**Mr. Atul Sharma**

(Lecturer)

Mechanical Engineering Department

Thapar University, Patiala

### Countersigned by

  
**Dr. S.K. Mohapatra**

Sr. Professor and Head

Mechanical Engineering Department

Thapar University, Patiala

  
**Dr. S.S. Bhatia**

Dean

Academic Affairs

Thapar University, Patiala

## **ACKNOWLEDGEMENT**

Completion of this thesis is carried out with the support of many people and their helpful assistance and references. First of all, I would like to express my sincere gratitude and indebtedness to my supervisor, Dr. S.S. Mallick, Assistant Professor in the Department of Mechanical Engineering of Thapar University, Patiala for his patient guidance, valuable suggestions, excellent advice and generous assistance.

I also wish to express my sincere thanks to Ms. Anu Mittal to carry out research and analysis work in right direction. I would like to convey special thanks to co-supervisor Mr. Atul Sharma and Mr. Gautam Setia who encourage me constantly, sharing their knowledge and experiences during the time of study.

I am also thankful to my colleagues for successful accomplishment of experimental work, performing of conveying trials throughout day, interesting discussions and other technical and social support. A special debt of gratitude is owed to the authors whose works I have consulted and quoted in this work.

The opportunity, support, exposure and atmosphere provided by the Thapar University, Patiala, to carry out my studies are highly appreciated. The financial support provided by the Department of Science and Technology (DST) and Council of Scientific and Industrial Research (CSIR) to carry out my studies is greatly appreciated.

Last but not least, I am forever grateful to my parents, family and friends for their unconditional support and best wishes.

## ABSTRACT

Pressure drop is very decisive and analytical parameter in the context of pneumatic conveying to know about flow characteristics and operating conditions for the reliable designing of fluidized dense phase pneumatic conveying systems. This study presents the results of ongoing investigation on transient pressure pulses using Shannon entropy technique. Pressure fluctuations (produced by gas-solid phase flow during fluidized dense phase conveying) were recorded by pressure transducers installed at strategic locations of pipeline. In the present work, two different powders have been conveyed i.e. fly ash (median particle diameter 45  $\mu\text{m}$ , particle density 1950  $\text{kg/m}^3$ , loose-poured bulk density 950  $\text{kg/m}^3$ ) and cement (median particle diameter 15  $\mu\text{m}$ , particle density 3060  $\text{kg/m}^3$ , loose-poured bulk density 1070  $\text{kg/m}^3$ ) through different pipelines (51 mm I.D. x 70 m long and 63 mm I.D. x 24 m long). The influences of superficial air velocity on Shannon entropy were also investigated.

In this study, transient nature of pressure fluctuations was taken into consideration (instead of steady state behavior) for investigation to know more about flow characteristics. It was found that value of Shannon entropy and standard deviation increased along the straight sections of pipe for both products and for different pipelines. However, there is a decrease in value of Shannon entropy after the flow through bend. Different range of Shannon entropy value was obtained for fly ash and cement. Higher value of Shannon entropy was noticed corresponding to low velocities and high velocity region while minimum value of entropy was found corresponding to medium velocities. Effect of solid mass flow rate on Shannon entropy at constant value of air mass flow rate was also observed.

## TABLE OF CONTENTS

	<b>Page No.</b>
CERTIFICATION	i
ACKNOWLEDGEMENT	ii
ABSTRACT	iii
TABLE OF CONTENTS	iv
LIST OF FIGURES	vi
LIST OF TABLES	ix
LIST OF SYMBOLS	x
<b>CHAPTER 1: Introduction and objectives</b>	<b>1</b>
1.1 Introduction	2
1.2 Objectives	4
<b>CHAPTER 2: Literature review</b>	<b>5</b>
2.1 Pneumatic conveying	6
2.2 Basic components of pneumatic conveying system	7
2.3 Modes of pneumatic conveying	9
2.4 Pressure models	11
2.5 Review of previous research work	12
2.6 Pressure signals	17
2.7 Signal processing techniques	18

<b>CHAPTER 3: Test facility and experimental procedures</b>	24
3.1 Experimental setup	25
3.2 Test product properties	28
3.3 Calibration procedure	29
3.4 Operational procedure	33
<b>CHAPTER 4: Investigation into pressure fluctuations</b>	35
4.1 Conveying cycle signals	36
4.2 Pressure fluctuations	37
4.3 Variation in Velocity and Density along the length of pipeline	41
<b>CHAPTER 5: Results and discussion</b>	44
5.1 Shannon entropy	45
5.2 Standard deviation	50
5.3 Effect of superficial air velocity	53
5.4 Effect of solid mass flow rate	58
<b>CHAPTER 6: Conclusion and future scope of work</b>	63
6.1 Conclusion	64
6.2 Future scope of work	65
<b>REFERENCES</b>	66
<b>APPENDIX: A1</b>	70
<b>APPENDIX: A2</b>	74
<b>COMMUNICATIONS</b>	77

## LIST OF FIGURES

	<b>Page No.</b>
<b>Figure 2.1:</b> Pressure drop caused by straight section and bend	10
<b>Figure 3.1:</b> Schematic Layout of the 54 mm I.D. x 70 m test rig	27
<b>Figure 3.2:</b> Piping and Instrumentation diagram for compressed air	28
<b>Figure 3.3:</b> Calibration curve for pressure transducer P4	30
<b>Figure 3.4:</b> Calibration curve for pressure transducer P6	31
<b>Figure 3.5:</b> Calibration curve for flow meter	32
<b>Figure 3.6:</b> Calibration curve for load cell	33
<b>Figure 4.1:</b> Signals obtained during conveying cycle	36
<b>Figure 4.2</b> Pressure fluctuations (P6 & P9) for fly ash (63.5 mm I.D. x 24 m long pipeline) ( $m_f = 0.052$ kg/s, $m_s = 4.2$ t/hr)	37
<b>Figure 4.3:</b> Pressure fluctuations (P6 & P9) for fly ash (63.5 mm I.D. x 24 m long pipeline) ( $m_f = 0.028$ kg/s, $m_s = 4.08$ t/hr)	38
<b>Figure 4.4:</b> Pressure fluctuations (P6 to P9) for fly ash (51 mm I.D. x 70 m long pipeline) ( $m_f = 0.029$ kg/s, $m_s = 4.4$ t/hr)	39
<b>Figure 4.5:</b> Pressure fluctuations (P6 to P9) for cement (63.5 mm I.D. x 24 m long pipeline) ( $m_f = 0.05$ kg/s, $m_s = 2.4$ t/hr)	40
<b>Figure 4.6:</b> Velocity difference versus solid loading ratio for fly ash	41
<b>Figure 4.7:</b> Density difference versus solid loading ratio for fly ash	43
<b>Figure 5.1:</b> Shannon Entropy versus pipeline length for fly ash	46

(63 mm I.D. x 24 m long pipeline) ( $m_f = 0.025 - 0.05$ kg/s; $m_s = 4 - 6$ t/hr)	
<b>Figure 5.2:</b> Shannon Entropy versus pipeline length for fly ash	47
(51 mm I.D. x 70 m long pipeline) ( $m_f = 0.016 - 0.039$ kg/s; $m_s = 2 - 4$ t/hr)	
<b>Figure 5.3:</b> Shannon Entropy versus pipeline length for Cement	47
(63 mm I.D. x 24 m long pipeline) ( $m_f = 0.015 - 0.038$ kg/s; $m_s = 4 - 7$ t/hr)	
<b>Figure 5.4:</b> Shannon Entropy versus pipeline length for Cement	48
(51 mm I.D. x 70m long pipeline) ( $m_f = 0.026 - 0.050$ kg/s; $m_s = 2 - 3$ t/hr)	
<b>Figure 5.5:</b> Standard deviation versus pipeline length for fly ash	51
(63 mm I.D. x 24 m long pipeline) ( $m_f = 0.025 - 0.05$ kg/s; $m_s = 4 - 6$ t/hr)	
<b>Figure 5.6:</b> Standard deviation versus pipeline length for fly ash	52
(51 mm I.D. x 70 m long pipeline) ( $m_f = 0.016 - 0.039$ kg/s; $m_s = 2 - 4$ t/hr)	
<b>Figure 5.7:</b> Standard deviation versus pipeline length for cement	52
(63 mm I.D. x 24 m long pipeline) ( $m_f = 0.015 - 0.038$ kg/s; $m_s = 4 - 7$ t/hr)	
<b>Figure 5.8:</b> Standard deviation versus pipeline length for cement	53
(51 mm I.D. x 70m long pipeline) ( $m_f = 0.026 - 0.050$ kg/s; $m_s = 2 - 3$ t/hr)	
<b>Figure 5.9:</b> Shannon Entropy versus length for fly ash at different velocity ranges	55
(63 mm I.D. x 24 m long pipeline)	
<b>Figure 5.10:</b> Shannon Entropy versus length for cement at different velocity ranges	55
(63 mm I.D. x 24 m long pipeline)	
<b>Figure 5.11:</b> Shannon entropy versus superficial air velocity for fly ash	56
(63.5 mm I.D. x 24 m long pipeline)	

<b>Figure 5.12:</b> Shannon entropy versus superficial air velocity for cement (63.5 mm I.D. x 24 m long pipeline)	57
<b>Figure 5.13:</b> Shannon Entropy versus length for fly ash at varying $m_s$ (63 mm I.D. x 24 long pipeline)	58
<b>Figure 5.14:</b> Shannon Entropy versus length for fly ash at varying $m_s$ (63 mm I.D. x 24 long pipeline)	59
<b>Figure 5.15:</b> Shannon Entropy versus length for cement at varying $m_s$ (63 mm I.D. x 24 long pipeline)	59
<b>Figure 5.16:</b> Shannon Entropy versus length for cement at varying $m_s$ (63 mm I.D. x 24 long pipeline)	60
<b>Figure 5.17:</b> Shannon entropy versus solid loading ratio for fly ash (63.5 mm I.D. x 24 m long pipeline)	62
<b>Figure 5.18:</b> Shannon entropy versus solid loading ratio for cement (63.5 mm I.D. x 70 m long pipeline)	62
<b>Figure A2.1:</b> Pressure fluctuations (P6 to P9) for cement (63.5 mm I.D. x 24 m long pipeline) ( $m_f = 0.023$ kg/s, $m_s = 2$ t/hr)	74
<b>Figure A2.2:</b> Pressure fluctuations (P6 to P9) for cement (51 mm I.D. x 70 m long pipeline) ( $m_f = 0.042$ kg/s, $m_s = 2.4$ t/hr)	75
<b>Figure A2.3:</b> Pressure fluctuations (P6 to P9) for fly ash (51 mm I.D. x 24 m long pipeline) ( $m_f = 0.042$ kg/s, $m_s = 4$ t/hr)	76

## LIST OF TABLES

	<b>Page No.</b>
<b>Table 3.1:</b> Physical properties of test products	29
<b>Table A1.1:</b> Shannon entropy values for fly ash (63.5 mm I.D. x 24 m long pipeline)	70
<b>Table A1.2:</b> Shannon entropy values for fly ash (51 mm I.D. x 70 m long pipeline)	71
<b>Table A1.3:</b> Shannon entropy values for cement (63.5 mm I.D. x 24 m long pipeline)	72
<b>Table A1.4:</b> Shannon entropy values for cement (51 mm I.D. x 70 m long pipeline)	73

## LIST OF SYMBOLS

I.D.:	Internal diameter of pipeline [m]
f:	Friction factor in pipeline
L:	Length of pipeline [m]
V:	Velocity of air [ $\text{ms}^{-1}$ ]
$d_s$ :	Particle size [m]
$d_{50}$ :	Median particle diameter [m]
$m_s$ :	Solid mass flow rate [ $\text{thr}^{-1}$ ]
$m_f$ :	Air mass flow rate [ $\text{kgs}^{-1}$ ]
$\rho$ :	Density of air [ $\text{kgm}^{-3}$ ]
$\rho_{bl}$ :	Bulk solid density [ $\text{kgm}^{-3}$ ]
$\rho_m$ :	Mean density of air [ $\text{kgm}^{-3}$ ]
$\rho_s$ :	Particle density [ $\text{kgm}^{-3}$ ]
$\lambda_f$ :	Air only friction factor
$\lambda_s$ :	Solids friction factor
$\lambda_{bs}$ :	Solids friction factor for bends
$\Delta P_b$ :	Pressure drop across bends [Pa]
$\Delta P_v$	Pressure drop in vertical section
$m^*$ :	Solid to gas mass flow rate ratio

# **CHAPTER 1: INTRODUCTION AND OBJECTIVES**

## 1.1 Introduction

Pneumatic transportation of bulk solids is gaining popularity for a wide range of applications in industries, such as power, petrochemical, agricultural, mineral industries etc. Proper design of the pneumatic transport system requires knowledge of the pressure drop, minimum conveying air velocity and flow mechanisms. Different types of flow modes occur in horizontal pipeline during positive pressure pneumatic conveying depending upon the material properties (e.g. particle diameter, bulk density and particle shape) and conveying parameters, such as superficial air velocity and loading ratio (Wypych, 1989). The conventional mode of conveying is known as dilute-phase (suspension-flow), where the velocity of the gas is sufficiently high to keep the particles suspended during the flow. Dilute-phase of conveying has limitations such as large sized compressor or higher energy consumption, higher chances of wear of pipes and bends, larger size of air-particle separator etc. In recent years, fluidized dense phase conveying of powders (Geldart A materials such as fly ash and cement) has become more popular. This mode of pneumatic transport takes advantage of the air retention properties of the bulk material (Mainwaring and Reed, 1987) with reduced gas flow rate, smaller size of pipeline, lower transport velocities and lower product degradation. However, determination of important design parameters such as pressure drop and minimum transport boundary of dense phase pneumatic conveying system is a difficult task for the researchers. (Mallick and Wypych, 2009).

Several models have been proposed by previous researchers to predict the pipeline pressure drop. These models are used to determine solid friction factor and associated pressure drop. Some models are based on the empirical approach developed by Stegmaier (1978), Weber (1981), Rizk (1982), Pan and Wypych (1992), Williams and Jones (2006). These models have limited

accuracy when they are applied to proper scale-up conditions (Mallick, 2010). These models used steady state data and mean values of parameters without considering the chaotic attribute of flow phenomenon and instantaneous changes in pressure and other parameters (particle velocity, air density etc).

The stochastic nature of gas-solid two phase flow evolved transient and random like pressure fluctuations (Dhodapkar and Klinzing, 1993). These pressure signals could be used to provide useful information about the flow characteristics and identification of specific conveying mode. Dhodapkar and Klinzing (1993) measured pressure fluctuation in power spectral density format and observed that distinct power spectral format is obtained for different flow regimes. Jama (2000) concluded that reduction of the gas velocity from the pressure minimum value would result in repeatable fluctuations at frequencies below 1 Hz. Hui Li (2002) analyzed wall pressure signals by wavelet multi resolution and then applied statistical analysis, e.g. Root mean square (RMS), skewness factor in frequency space. Pakh (2006) applied phase space analysis, power spectral density, rescaled range analysis, wavelet analysis to investigate into time series pressure signals produced in dilute phase conveying. Jaboon et al. (2013) proposed that average frequency and average intensity of Power Spectral Density decreased with a decrease in superficial air velocity. Recently, Mittal (2015) employed three techniques of signal processing to investigate into pressure fluctuation and found an increment in the value of Shannon entropy, decrease in the value of Hurst exponent and increased area of the phase space diagram along the direction of flow through the straight sections of the pipeline.

In recent years, a new technique has begun for the analysis of transient pressure fluctuations based on computation of Shannon entropy dependent on time. The Shannon entropy is a

measurement of information content and predicts the degree of uncertainty in the outcome of an event (Shannon, 1948). Liang (2007) performed the Shannon entropy analysis of pressure fluctuations in dense phase pneumatic conveying of pulverized coal to reveal the flow characteristics. Duan and Cong (2013) applied the concept of Shannon entropy to identify flow patterns and to predict the uncertainty level in the dynamic behavior of the two phase flow using Geldart group B and Group D particles. Recently, Mittal (2014) investigated into pressure fluctuations generated from dense phase pneumatic conveying of fine powders such as fly ash and white powder. From the above study, it is found that relatively few attempts has been made to investigate into pressure fluctuations in horizontal pneumatic transport, especially for fine powders compared to the large amount of work performed in the field of fluidization and coarse particle flows in dilute phase flow. Therefore, in the present work, efforts have been made to investigate into the pressure fluctuations for fine powders and validate some of the recent findings against new experimental data.

## **1.2 Objectives**

Specific objectives include:

- I. Investigation of pressure fluctuation along the length using Shannon entropy and standard deviation for cement and fly ash in different pipelines.
- II. Influences of superficial air velocity on the flow characteristics by study the variation in Shannon entropy along the length caused by changes in superficial air velocity.
- III. Study the effect of solid mass flow rate or solid loading ratio on Shannon entropy related to pressure fluctuations from dilute to dense phase.

## **CHAPTER 2: LITERATURE REVIEW**

This chapter presents the efforts carried out by different researchers in the field of signal processing techniques is being used to study the pressure fluctuations or pressure signals obtained by using pressure transducer during pneumatic transport of bulk solids. Previous researchers also did an investigation of pressure fluctuations in the area of fluidization and pneumatic conveying using these techniques. So, some review is taken on these studies to understand the concepts, suitable conditions and relevancy of these techniques.

## **2.1 Pneumatic Conveying**

Pneumatic conveying of bulk solids is a material transportation process, in which bulk particulate materials (cement, fly ash, flour, chocolate powders) and granular products (crushed coal, grain, sugar) are moved over horizontal and vertical distances through the confined flow channel with the help of a compressed or vacuum gas stream. Using either positive or negative pressure of air or other gases, the material to be transported is forced or sucked through pipes and finally separated from the carrier gas by using a cyclone separator etc. and deposited at the desired destination. A well designed pneumatic conveying system is often a more practical and attractive method of transporting materials than mechanical systems such as belt, screw, drags conveyors and others (Klinzing, 2009).

Merits of pneumatic conveying are:

- Low Maintenance and manpower costs
- Flexibility in routing by using the elbows and bends
- Materials can pick from several areas and can distribute to several areas

- Toxic products can transport without affecting the environment.
- Good Security due to proper enclosed flow channel (pipeline) used to convey the valuable products like diamond ore.
- Easy to automate and control pneumatic conveying systems, product flow rates can be monitored continuously.
- Greater Capacity: Solid Particles such as pulverized coal, cement, and corn can be transported efficiently at large conveying rates (e.g. 100 - 400 t/h)

Demerits of pneumatic conveying are:

- Relatively high power consumption
- Wear and abrasion of equipment
- Limited conveying distance
- Incorrect design can result in particle degradation
- Due to complex flow in pneumatic conveying, high level of skill is required to design, operate and maintain the system

## **2.2 Basic components of pneumatic conveying system**

A pneumatic conveying system consists of four main groups of basic components and need to be matched carefully to obtain a successful conveying system. The four main groups are:

### *1) Prime Movers*

In the pneumatic conveying system, gas acts as conveying medium for the transportation of bulk materials from one place to another. Wide range of compressors, blowers, fans and vacuum pumps are available to supply gas depending upon the application. The prime movers are also associated with drying and filtering unit.

### *2) Feeding Device*

The method of introducing the solid into flowing gas stream is critical because of majority of conveying system problems occurs due to mismatch of feeder characteristics to the pipeline conveying characteristics. According to Klinzing (2009), there is large change in momentum when solids are mixed with flowing stream. Selection of feeding device is such that it meets with requirements of solids as well as system requirements. Commonly used feeding devices with their pressure ranges are:

- a) Rotary valves – low pressure (maximum 100 kPa)
- b) Screw feeders – medium pressure (maximum 300 kPa)
- c) Venturi feeder – low pressure (operates up to 20 kPa)
- d) Blow tanks – high pressure (maximum 1000 kPa)

### *3) Conveying Line*

This consists of straight pipelines (horizontal and vertical), bends, expansions, flanges or couplings, valves, etc. The selection of piping material will depend upon the factors such as the pressure requirement, product abrasiveness and product physical properties.

#### *4) Gas-solids separation devices*

Material needs to be separated from the gas stream. For this purpose, bag filters or cyclone separators are used. The selection of a particular type of feeder depends upon a number of factors, the primary factor being the size of solid particles.

### **2.3 Modes of pneumatic conveying**

Pneumatic conveying systems can be categorized into various flow modes. The two main categories are:

- a) Dilute phase conveying
- b) Dense phase conveying

Each flow mode can be categorized on basis of solids to air mass flow rate ratio ( $m^*$ ) which is referred as the “solids loading ratio”. Dilute phase conveying is thought of as a fully suspended flow and generally employs large volume of gas at high velocities. Dense phase flows can be defined as those in which conveyed material completely fills sections of pipeline and also called by non-suspension flow.

The capability of a pneumatic conveying system to achieve a given product mass flow rate depends on diameter of the pipeline, distance to be conveyed and maximum pressure available for conveying. Due to several reasons such as friction between particles and particle-wall, pressure decreased and solids cannot flow over desired distances. That is why the measurement of total pipeline, air pressure drop is considered as one of the most important aspects of the pneumatic conveying design system. To determine the pressure drop, two separate techniques can be used. One is used for horizontal and vertical straight pipe sections and other one is used for bends, valves or any other sections of pipe. (Pan, 1992)

*Estimation of pressure drop in straight sections of pipe and bends separately*

In pneumatic conveying, conveying conditions like air velocity, air density, particle velocity, vary along the pipeline due to compressibility of conveying gas and this conveying conditions can affect the pressure drop. Hence, for accurate determination of total pipeline, air pressure drop, bends and straight sections of pipe are to be separately dealt with.

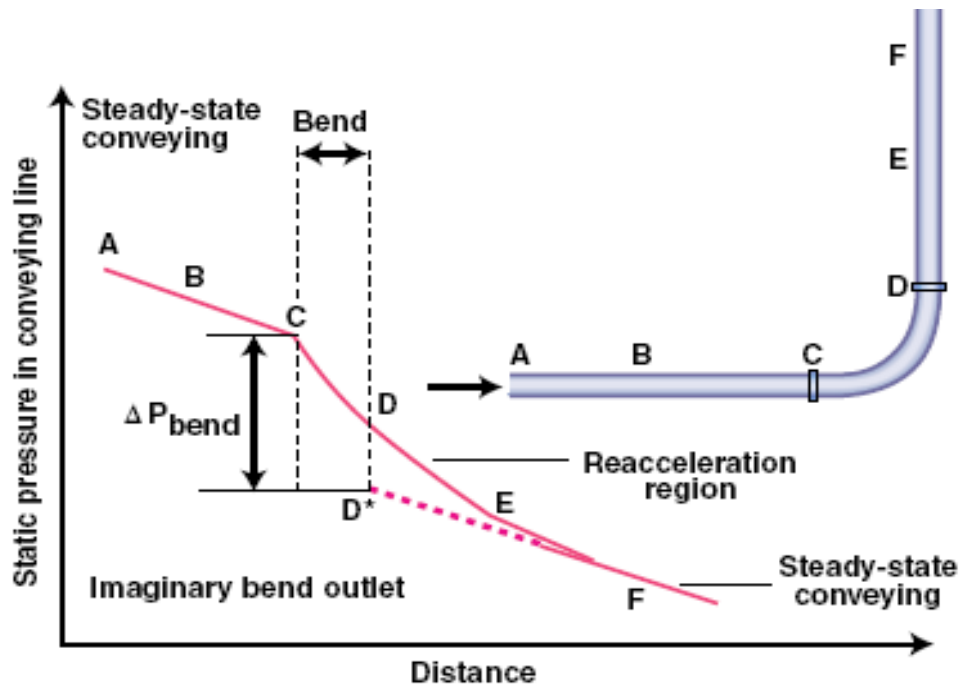


**Figure 2.1:** Pressure drop caused by bend and straight section (Dhodapkar and Klinzing, 2009)

Various Theoretical models are developed to predict the total pipeline pressure drop. However, the established theoretical correlations are used only with restricted conditions (e.g. the particles are coarse, rigid and conveyed in dilute phase). Mallick (2010) refers that Barth (1958) is one of the earliest researchers who proposed that pressure drop determination due to air-solid mixture is the sum of two components of pressure drop due to air only and pressure drop due to solids only.

Acceleration losses and vertical losses are as proposed by Marcus et. al (1985) and Marcus and Chamber (1986).

$$\Delta P = (\lambda_{f+} m^* \lambda_s) L/D \rho_f V^2/2 \quad (\text{Barth, 1958}) \quad (1)$$

$$\Delta P_{\text{accel}} = m^* \rho_f V \quad (\text{Marcus, 1985}) \quad (2)$$

$$\Delta P_v = m^* \rho g \frac{L}{V} (\text{Chamber and Marcus, 1986}) \quad (3)$$

## 2.4 Pressure drop models

### *Pressure drop due to air only*

Formulae that were developed by experiments are for incompressible fluid such as water and the inner surface conditions of straight pipe and bend remain constant are widely used to predict the pressure drop due to air alone. In pneumatic conveying, the compressibility of air changes significantly and inner conditions of the pipe changes also with time and wear due to the striking of particles and depend on flow whether it is laminar, transitional or turbulent flow. Hence the applicability of these formulas is not valid and would not give accurate estimates of pressure drop. Formulae based on incompressible flows are modified to allow the effect of compressibility to estimate the accurate value of pressure drop. Generally, the determination of pressure drop due to air alone in straight sections of pipe can be given by Darcy-Weisbach's equation

$$\Delta P_a = 4\rho_a f L V^2 / 2D \quad (4)$$

### *Pressure drop due to solid only*

Different types of forces act on solid particle when it conveys in horizontal or vertical pipe. These forces are Drag Force, friction force between particle and pipe wall, resistance which hinder the motion of particles due to gravity in a vertical pipe. The gravity force is not an influential parameter in horizontal pipe when particle velocity is more than the saltation velocity.

By using the Euler Momentum equation, balances the different forces of both air and solid and assuming the isothermal conditions. To find out the pressure drop due to solid only, value of  $\lambda_s$  need to find out which is a function of various parameters such as particle density, pipe roughness, particle shape factor, friction coefficient between pipe wall and solids, pipe diameter and length. By using the dimensional analysis, expression of  $\lambda_s$  can develop and find out pressure drop due to solid only. (Pan, 1992)

## **2.5 Review of previous research work**

Tsuji and Morikawa (1982) classified the flow patterns depend on air and particle flow rate and linked the pressure fluctuations with the flow pattern especially at low air velocities. It was found that pressure fluctuation increases with decrease in air velocity at low air velocities range due to changes in flow pattern from dispersive to fluctuating one and formation of particle cluster. The effect of particle diameter was also noted on the amplitude of pressure fluctuations and suggested that behavior of pressure fluctuations was different for both different diameter particles at low velocities. Waveform analysis of pressure fluctuations was also done and made some plots showed deviation in Gaussian type distribution for pressure fluctuations at low air velocities and negative skewness compared to positive skewness at high air velocities.

Dhodapkar and Klinzing (1993) studied the pressure fluctuations generated in pneumatic conveying of solids in horizontal pipes and represent it in a power spectral density function (PSDF) to observe and identification of the flow pattern. They studied the pressure fluctuation in single phase flow and effect of solid flow rate on pressure drop due to single phase flow. Higher frequency pressure fluctuations decrease with a decrease in gas velocity. They concluded that at same gas velocity, addition of solids increase the magnitude of low frequency fluctuations by absorbing the higher frequency fluctuations. Reduction in gas velocity changed the flow pattern from homogenous to dune flow through stratified flow, blowing packets. Static pressure transducers reliable for homogenous flow and differential pressure transducer were preferred for dune/slugg flow because of lack of susceptibility towards upstream and downstream conditions.

Plasynski, Klinzing and Mathur (1994) estimated the pressure drop in high pressure vertical pneumatic transport. Pressure drop in vertical section consists of several factors:

- Pressure drop due to acceleration of particles entering the vertical pipe ( $\Delta P_a$ ).
- Frictional pressure losses due to solids and liquids ( $\Delta P_f$ ) and static head ( $\Delta P_s$ )
- Pressure drop due to static head Pressure drop due to other external forces (such as electrostatics) ( $\Delta P_{add}$ ).

They also discussed the effect of particle size, particle density, solid feed rate, gas density on pressure drop. Pressure drop for large particles would be greater than smaller particles. More energy was required to suspend and lift the heavier particles. Pressure drop increased with increase in particle density, solid flow rate due to voidage decreases and pressure drop due to static head and friction increase.

$$\Delta P_s = \rho_p (1-\epsilon) L_g + \rho_f \epsilon L_g \quad \text{Where } \epsilon \text{ is voidage between particles} \quad (5)$$

Pan (1999) used the loose poured bulk density and particle mean diameter to select the flow mode for a particular material. In general three flow modes was observed, (1) smooth transition from dilute to fluidized dense phase, (2) dilute-phase, unstable zone and slug flow (3) dilute phase only. Pneumatic conveying characteristics of these flow modes were plotted between the pressure drop and air mass flow rate. Pan proposed that pressure drop decreased with decreasing air mass flow rate and reached a minimum value before again increasing with higher rate. Different flow mode occurs in various types of material like powders (fly ash) light granular products (wheat, rice) and heavy granular products (crushed coal) depending upon the value mass flow rate, pressure drop.

Jama, Klinzing and Rizk (2000) investigated the flow patterns and pressure fluctuations near the minimum pressure point and unstable zone where steady state range minimized during the pneumatic conveying of polymer pellets. Pressure peaks were observed as the gas velocities reached at minimum pressure and leads the system towards unstable zone characterized by subsequent oscillations. It also suggested that abrupt changes in pressure peaks indicate that system was operated in unstable zone. An Increment in the solid flow rate at a high gas velocity caused a rise in pressure peaks because of interaction between gas and solid high energy (due to high velocity) conveying mode. Unstable flow also linked with differential pressure fluctuations by normalizing (divide with average pressure drop) the range of pressure fluctuations and found that value increase significantly as the flow becomes unstable.

Ommen et al. (2004) suggested the placement of probes for estimation of dynamic pressure measurements in large scale-fluidized beds. Pressure fluctuation was measurable in limited areas of the bed, local pressure detected up to a radial distance of about 0.5 from their origin but not more than 1.5m from their origin. There was need of multiple transducers to cover whole bed to

measure the pressure fluctuation. Pressure fluctuations consisted of low-amplitude compression waves due to bubble passage and high-amplitude compression waves due to bubble coalescence and bubble eruption. They concluded that probe dimensions and probe spacing were very important because their magnitude was going to decrease at some distance from their origin. For Geldart B particles, radial spacing of pressure probe should not exceed 1m. Probes should be at height of 30% to 40% of bed height.

Williams et al. (2008) investigated pressure fluctuations in dense phase pneumatic conveying of powders and suggested that flow mechanisms in this type of conveying mode are transient in nature rather than steady state. Analysis was done by calculating pulse velocity and its frequency and found out an increment in pressure fluctuation along the pipeline. This analysis proposed that gas expansion is a crucial factor in increase in amplitude of pressure fluctuations.

Mallick (2009) estimated the minimum transport boundary in dense phase pneumatic conveying and developed a new design procedure based on the Froude number at entry to the pipe. It was also discussed that reduction in gas flow rate beyond the good steady state condition would lead to formation of unsteady dunes with rise in pressure fluctuations and further decrease in gas flow rate may cause blockage in pipeline. Boundary from where the system was unable to transport the material was defined as an unstable boundary or minimum transport boundary which characterized by rapid increase in pressure fluctuations. White powder, fly ash and ESP dust were conveyed in pipeline to obtain the experimental data and calculated minimum Froude number range 3 to 5.7 at the pipe inlet as required minimum transport conditions. It is concluded that Froude number can be an important and useful parameter in determining minimum transport conditions.

Behera et al. (2013) analyzed fluidized dense phase pneumatic conveying by solving the steady state flow equation written for different phases by assuming flow parameters in those equations depend upon particle size distribution of conveying material and tried to find maximum possible distance of conveying. Scale up analysis was also conducted for pipeline diameter and length under different flow conditions. Pressure drop coefficient and power consumption coefficient were calculated for different solid loading ratio and showed that pressure drop coefficient remain constant for low solid loading ratio ( $m^* = 15$ ) but rise in power consumption coefficient occurred due to increment in air velocity and for higher solid loading ratio, pressure drop coefficient increased due to rise in contribution of pressure drop due to air alone along the length of pipeline and power consumption remained constant because of insignificant change in superficial air velocity during the flow.

Liang et al. (2014) developed the correlations of pressure drop through the bends and investigated the effect of pipe diameter  $D$ , pipe centerline radius, bend geometry (bend radius ratio), location (vertical upward, vertical downward, horizontal). Pressure drop was least in vertical downward bend because gravity accelerated the flow and overcome the resistance. Pressure drop value was higher in vertical upward bend because gravity opposed the flow and consumed more energy to suspend the particles in pipe. In horizontal bend, suspended velocity was very less and due to same height level pressure drop due to rising of particles was ignored. Pressure drop was less in short radius bend compare to long radius bend because the short radius bend takes the abrupt losses quickly while the long radius carries an unsteady condition over a long distance. As the gas-solid mixture entered the bend, some particles striking the bend wall and change their directions leads to particle-particle collision. Due to these collisions, Particle velocity decreased at bend but afterward acceleration at outlet of bend causes pressure drop.

**2.6 Pressure signals:** Solid-gas transport has an inherent ability to produce pressure fluctuations. Pressure Fluctuations also can be produced by variation in solids flow rate or unsteady flow from feeder, due to nature of air supply (pulsations caused by different types of compressors), flow around the bends, material Transport. So, all these types of pressure fluctuation make the procedure difficult to measure the pressure fluctuations due to solid transport. Pulsations or pressure fluctuations caused by compressor can be avoided by using regulators, surge tank and valves. Pressure fluctuations produced by feeder which introduce the solids into the system and fluctuations depend upon feeder RPM and ability of conveying air to pick up the solids. So, perfect steady flow is required to prevent the fluctuations and this can be achieved by using the extra length of tube or feed tee. Due to feed tee, solids dampened the feed fluctuations.

#### *Apparatus to measure the pressure signals*

Dhodapkar (1993) said that pressure fluctuations in two phase flow system give much information about flow conditions in flow line. Static pressure transducer and differential pressure transducer are used to measure the pressure signals. Differential pressure transducer measures the pressure fluctuation generated between the two tapping points. Mallick (2010) suggested that differential pressure transducer should be away from static transducers. Pressures signals can be measured by locating the pressure transducers on top or at the bottom of the pipe. At saltation velocity, signals are different from the bottom tap due to its tendency to get clogged. So, there is no requirement to measure the pressure signal from the bottom of the pipe. However, in this study, static pressure transducers are used to measure the pressure fluctuations.

Schempp (1973) proposed the system for measuring the pressure in a pipe in which solids are transported. Single inlet of primary gauge was connected to the transport line by a tube whose outlet was preceded by a first filter. A differential pressure limit gauge had one inlet connected to the line whose outlet was preceded by a first filter. A differential pressure limit gauge had one inlet connected to line by a similar filter and other inlet connected to outlet of first tube so as to measure the pressure drop across the first filter and indicates when either filter may be clogged. One attempted solution was to the plugging problem had been to interpose a flexible diaphragm between pressurized line and a sealed chamber in which gauge or other sensing device connected.

## **2.7 Signal processing techniques**

Many signal processing methods have been developed for the analysis of signals. Pressure signals generated by pressure transducers located at different locations of pipeline analyzed by these signal processing techniques. By taking transient nature of pressure signals into consideration, these techniques are more accurate for prediction of pressure drop, conveying parameters and about flow pattern. Assumption of steady state flow behaviour or average values by previous researchers has given inaccurate values of predicted conveying parameters.

Behera et al. (2012) did transient parameter analysis of fluidized dense phase pneumatic conveying and suggested that flow mechanism in this type of pneumatic conveying was highly transient and pulsatile rather than steady state behavior. These fluctuation signals characterized by pulse parameters like amplitude and frequency. Changes in these parameters analyzed and described that how the flow mechanism changed during the flow along the length of pipeline depend on initial velocity of pipeline and aeration or de-aeration rate of material bed. It was also

concluded that beginning with dense phase flow at inlet of pipeline, flow can change into dilute phase or remain as dense phase towards the end of pipeline.

Pahk (2006) discussed the various techniques based on frequency domain, time domain and phase space and used those techniques to develop some methods to identify the flow conditions from pressure fluctuations for different configurations, materials and decompose the original signal by using wavelet analysis to know contribution of various components (blower, feeder and noise signal) in pneumatic conveying setup. Power spectral analysis also applied for investigation of pressure fluctuations and resulted that power is decreased as solid flow rate increased.

#### *Power spectral analysis*

Power spectral density (PSD) is frequency domain characteristic of time series, can be obtained by fast Fourier transformation (FFT). Jaboon et al. (2013) used the power spectral density method of pressure fluctuations to investigate the characteristics of fluidization and to find out the effect of flow in various fluidization regimes like slugging regime, multiple bubbling regime, turbulent regime and homogenous dilute transport regime. It is proposed that average frequency and average intensity of PSD decreased with a decrease in superficial air velocity and concluded that PSD is an efficient method to evaluate performances in the industry. Dhodapkar and Klinzing (1993) used power spectral density function for wall pressure signals at different gas velocities and identified the flow pattern in pipeline. The disadvantage of this technique is that it cannot relate the frequency of pressure fluctuations with time at which particular flow mechanism is identified (which frequency is coming out of particular flow pattern).

### *Wavelet analysis*

Wavelet analysis is a time-frequency representation of continuous signals (analog signals). Information in multi-phase flow can be extracted by wavelet analysis and it is more suitable for unsteady flow than Fourier analysis and physical spaces. Renet. al. (2006) studied the behavior of fluidized bed by wavelet analysis and decomposed the original signal to know about the transition from dense phase to dilute phase. Hui Li (2002) analyzed data of wall pressure fluctuation signals in gas solid two phase flow by wavelet multi resolution and then some statistical analysis applied in frequency space. Based on wavelet analysis, suspension and dune flow extracted from random like pressure fluctuations. Signals having sharp changes can be better analyzed by using an irregular wavelet. (Behera, 2012).

### *Shannon entropy*

Entropy stands for “disorder or uncertainty”. Shannon Entropy is average amount of information in message signals (information signals, events, samples). It depends upon the occurrence of an event and justifies the determinacy of the outcome of that event. The frequency of a certain event or sample is more than others indicates decrease in Shannon entropy and make the data less informative. Shannon entropy quantifies the complexity of the dynamics; it should increase when the chaotic behavior is developed. That’s why Shannon entropy is the important tool to study the dynamic behavior associated with flow pattern of gas-solid two phase flow. Some work has been done by previous researchers on pressure fluctuations produced in fluidized bed and pneumatic conveying of coarser particles. So, some more review of previous work based on Shannon entropy is presented here.

Zhong et al. (2009) did Shannon entropy increment analysis of differential pressure fluctuations of a biomass fluidized bed to know about dynamic behavior of gas-solid phase flow and different flow patterns in fluidization bed. It was proposed that Shannon entropy increment analysis were very helpful to understand the random nature of gas-solid phase flow. Flow patterns were classified into three patterns: under fluidization, steady fluidization and turbulent fluidization. The Shannon entropy increment was lowest in steady-fluidization, while the Shannon entropy increment was highest in turbulent-fluidization. The pressure fluctuations were much more random in the turbulent fluidization than steady-fluidization and under-fluidization and system appeared random nature. With rise in superficial air velocity, rise in Shannon entropy increment occurred. Maximum increment took place in turbulent fluidization indicated that this flow pattern was more vulnerable to rise in chaotic nature with an increase in superficial air velocity.

Liang (2012) performed the Shannon entropy analysis of pressure fluctuations in dense phase pneumatic conveying of pulverized coal to reveal the flow characteristics and investigated the influence of differential pressure, moisture content and gas volume rate. The relation between Shannon entropy and pressure fluctuation, Shannon entropy and mass flow rate are established. It is proposed that the Shannon entropy value decreased first then increased considerably with increase in superficial air velocity under constant mass flow rate. Value of Shannon entropy decreased as the moisture content of coal increased. It was also noticed that conveying differential pressure influenced the Shannon entropy. Shannon entropy value increased by differential pressure and both values decreased with rise in moisture content.

Duan and Cong (2013) analyzed pressure fluctuations resulting from non uniform flow behavior of solid particles (Geldart B group and Geldart D group type particles in this work) in fluidization bed. Flow patterns (bubbling fluidization, turbulent fluidization, fast fluidization) in fluidized bed and transition between them with increase in superficial air velocity were identified by calculating the Shannon entropy of pressure fluctuations in fluidization bed. A comparison of both types of particles was also done which showed different behavior with respect to increasing superficial air velocity. Shannon entropy increased with increase in superficial air velocity in case of bubbling fluidization and reached to maximum value during transition from bubbling to turbulent fluidization. In Geldart B group type particles, this phenomenon happened very steadily, but in Geldart D group, this occurred slowly during initial fluidization and then rapidly reached to the maximum value as air velocity was increased. After reaching to maximum value, constant entropy, phase came which indicated that gas and particle continued to maintain intense interaction during turbulent fluidization. Bubbles disappeared with decrease in Shannon entropy value and this phenomenon identified as fast fluidization.

The Mittal (2014) applied Shannon entropy technique on pressure fluctuations generated during dense phase conveying of fly ash and white powder and found that Shannon entropy value and standard deviation increases along the straight section of pipeline in the direction of flow from the inlet of pipe to the exit of pipe. It was said that this could be happening due to rise in turbulence characteristics of flow along the pipeline. Overall value of Shannon entropy was increased along the length of pipeline. However, value of both (Shannon entropy and standard deviation) decreased during flow after the bend due to deceleration of particles through the bend. Non suspension nature of flow at the beginning of pipe could be the reason of the low value of Shannon entropy at inlet of pipe.

Mittal (2015) investigated flow mechanisms in dense phase pneumatic conveying by using three different signal analysis techniques. These techniques were rescale range analysis, phase space method and Shannon entropy. The investigation resulted that there was a decrease in overall value of Hurst exponent, an increase in area covered by phase space diagram and an increase in overall value of Shannon entropy with increase in conveying distance and explained that this was an indication of increase in degree of complexity of flow mechanism along the length of conveying pipeline. All three methods showed reverse trend of change during flow through the closely coupled bend due to dampening of turbulence or reduction in velocity of particles as particles approach towards bend. It is found that accuracy of Hurst exponent depend on the length of time series or number of data points. Calculation of Hurst exponent was more accurate for large number of data points series compared to short series.

**CHAPTER 3: TEST FACILITY AND EXPERIMENTAL  
PROCEDURES**

### 3.1 Experimental Setup

Pneumatic conveying trials were conducted in the pilot plant available in “Particle and Bulk Solids Technologies Laboratory installed at Thapar University (India) using fly ash and cement with different pipeline configurations. The test rig has been designed with the objective of handling research activities of main transport modes, i.e. dilute phase and dense phase conveying. For this, all experiments were performed for wide range of air flow rate and blow tank initial pressures through pipelines with different configurations like (different diameters and different lengths). Typical schematic for 54 mm I.D. x 70 m length is shown in Figure 3.1.

Compressed air was supplied using a rotary screw compressor (Make/Model: Kirloskar/KES 18-7.5) having the maximum delivery pressure of 750 kPa and flow rate of 202 m<sup>3</sup>/hr (Free Air Delivery). Different air flow rates (0 to 0.06 kg/s) were obtained by using an air flow control valve installed in compressed air line. A vortex flow meter was installed in the compressed air line to measure the air flow rates. Bottom-discharge blow tank (having 0.2 m<sup>3</sup> empty volume) with a maximum working pressure of 400 kPa was used for feeding the material into the pipeline. Blow tank was operated with three solenoid operated dome type valves (inlet, outlet and vent valves). 0.7 m<sup>3</sup> capacity receiving hopper was installed with bag filter (having reverse pulse jet type cleaning mechanism) at its top to separate material from the air stream. Shear-beam type load cells were attached to blow tank and receiving bin for measurement of solid mass flow rate. Different pipeline configuration (i.e. different diameter and length) were used to convey the materials such as 51 mm I.D x 24 m long and 63.5 mm I.D x 24 m long. All pipelines included a 3 m vertical lift and had 4 nos. of 90° bends of 1m radius of curvature.

Long sight-glasses (two sets of 300 mm) made of borosilicate glass for flow visualization (and to visualize the blockage phenomenon) were installed in pipeline at strategic locations. Five static pressure transducers (P4 and P6 to P9) (manufactured by Endress & Hauser, model: Cerabar PMC131, pressure range: 0-2 bar, maximum pressure: 3.5 bar (absolute) were located at various positions of pipeline. P4 was used to measure the total pipeline pressure drop and all other transducers were used to measure the pressure drop along the pipeline. Data from the electrical output signals from the load cells (voltage signals), pressure transducers and flow meter (current signals) were obtained by a PC compatible data Logger having 16 different channels with 14 bit resolution.



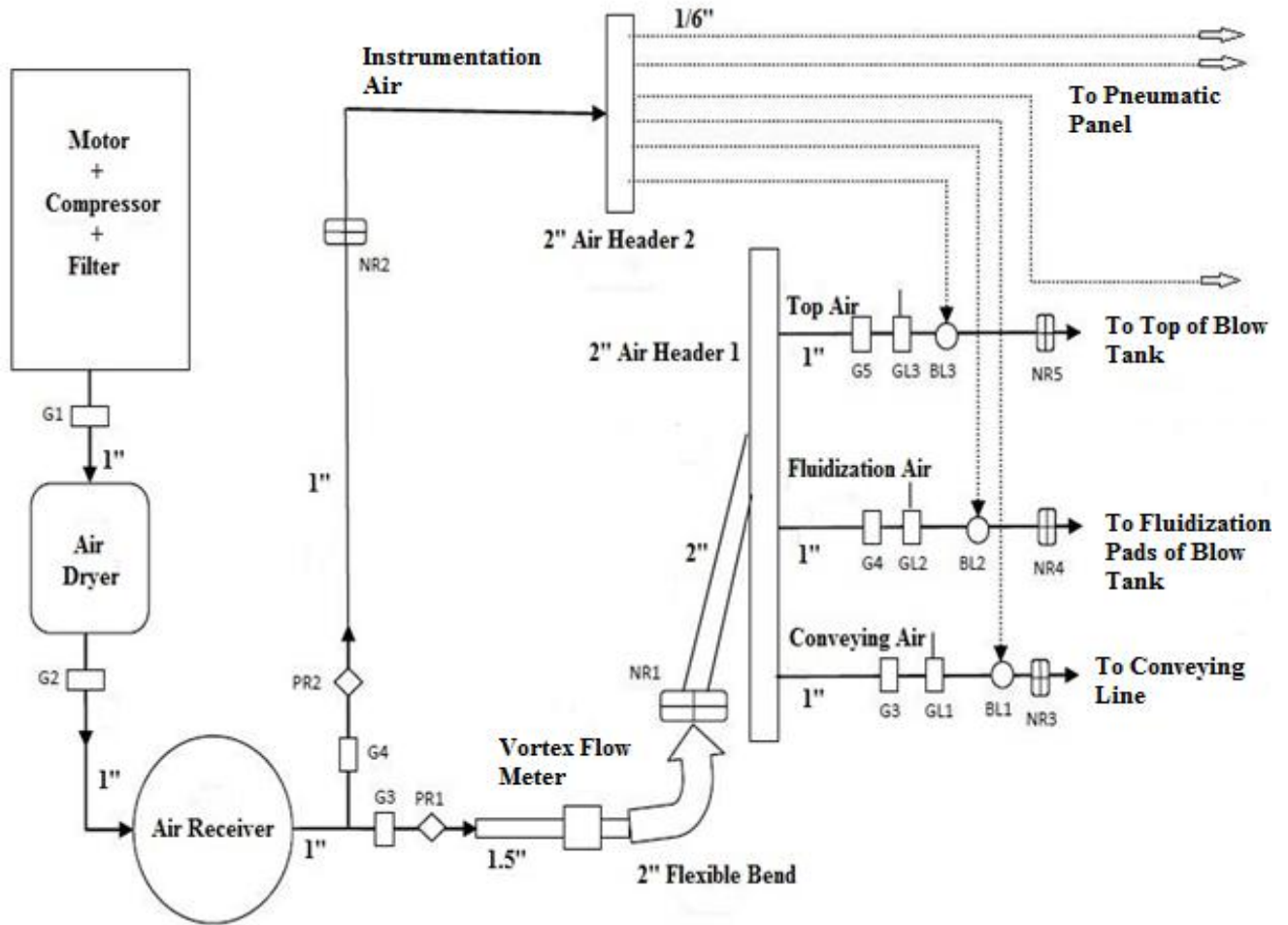


**Figure 3.2:** Piping and Instrumentation diagram for compressed air of 63.5 mm I.D. x 24 m Test Rig (for fly ash)

### 3.2 Properties of Test Product

Particle density was measured using water displacement method and particle size distribution was determined using laser diffraction analyzer. Physical properties of these products are listed in Table 1.

**Table 1: Physical properties of test products**

<b>Product</b>	<b><math>\rho_s</math></b> <b>(kg/m<sup>3</sup>)</b>	<b><math>\rho_{bl}</math></b> <b>(kg/m<sup>3</sup>)</b>	<b><math>d_{50}</math></b> <b>(<math>\mu\text{m}</math>)</b>
Fly Ash	1950	950	45
Cement	3060	1070	15

### **3.3 Calibration Procedure**

Load cells, pressure transducers and flow meter were calibrated using standard calibration procedure as described by Mallick (2010). All the pressure transducers were calibrated by maintaining constant static pressure in the conveying pipeline using blind flange and simultaneously recording the pressure signal from data logger. The standard calibration procedure for pressure transducers is given below:

- a) Pressure transducers have been installed at desired locations along the pipeline and connect these to data logger.
- b) Pipeline upstream of the receiver bin was closed using blind flange.
- c) The pipeline was checked for air leakages, rectify if any leakage found and open the vent valve to release the air from pipeline.
- d) Desired pressure value was adjusted by using the pressure regulator (e.g. 50 kPa) and opened the conveying pipeline valve.
- e) After that, pressure in the pipeline was measured using pressure gauge and recorded the pressure of all the transducers simultaneously from data logger.

Step (e) was repeated by adjusting the pressure regulator to different pressure readings.

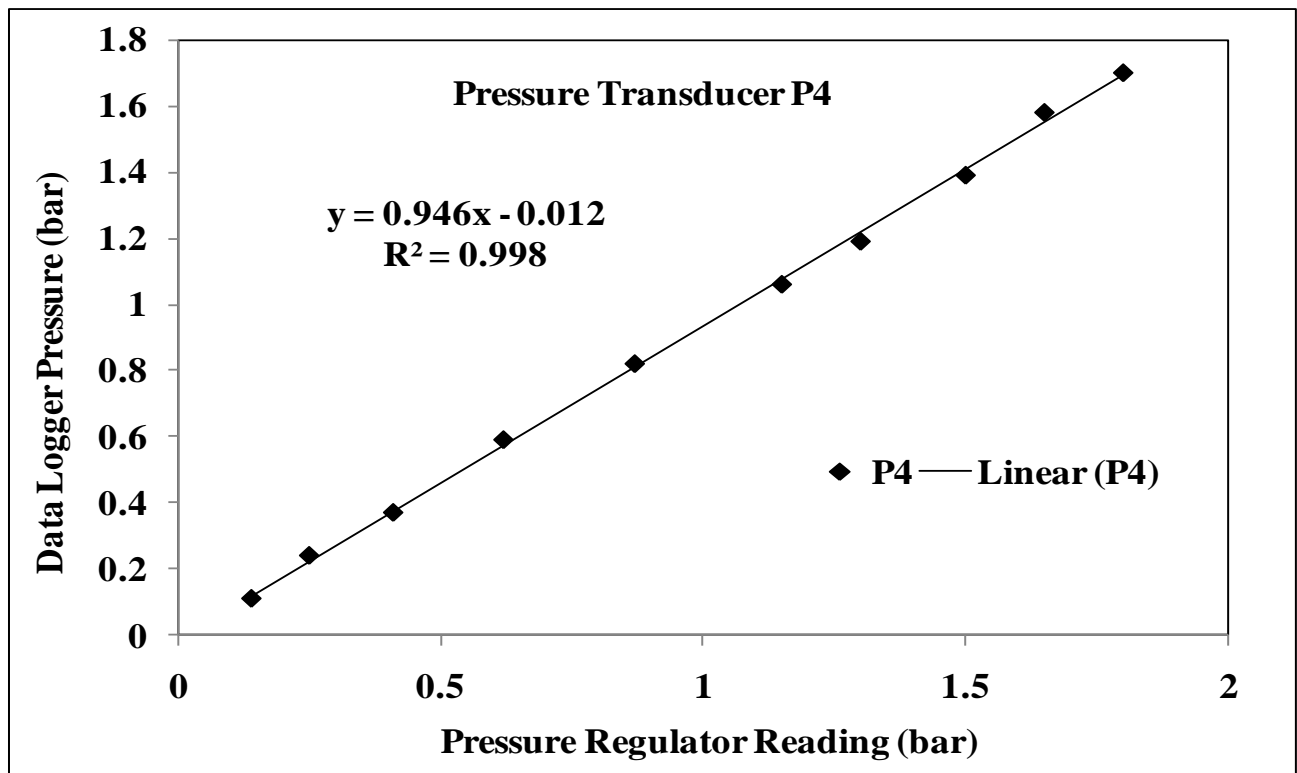


**Figure 3.3:** Calibration curve for pressure transducer P4

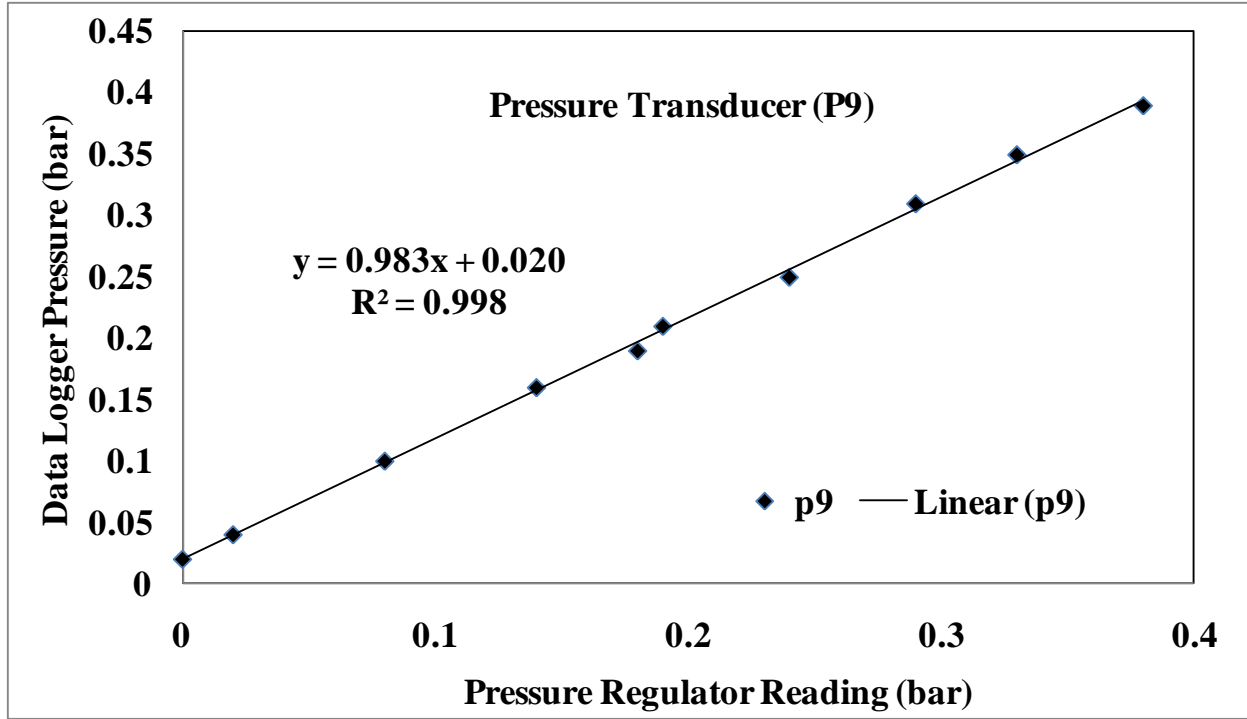


**Figure 3.4:** Calibration curve for pressure transducer P9

Flow rate of supply air in a conveying cycle was measured by using the vortex flow meter. This flow meter had a digital display which showed the reading of volumetric flow rate of air, at the same time it also generated an analog signal, which was fed to the data logger and after further processing of signal, data logger also displayed the volumetric flow rate. To calibrate the flow meter a continuous supply of air was conveyed in pipeline and readings of flow meter were recorded simultaneously at its digital display and at data logger. Pressure data at inlet flow meter was recorded with the help of pressure transducer to calculate density of inlet air to flow meter, so that its mass flow rate can be obtained.

Load cells were used to calculate the mass of material accumulated in and discharged from receiver bin and hopper. Blow tank and receiver bin were placed on shear beam type load cells.

Each load cell has maximum load bearing capacity of 500 kg. Such four load cells were used to carry combined weight of blow tank and material, receiver bin and material. Output from these four load cells was combined to give total load shared by each cell. The load cells generated a differential output voltage signal, which was fed into data logger to calculate corresponding weight. Two such combinations were used to measure the material discharge rate. To calibrate load cells, a known weights put on the structure and its value was recorded in the data logger.

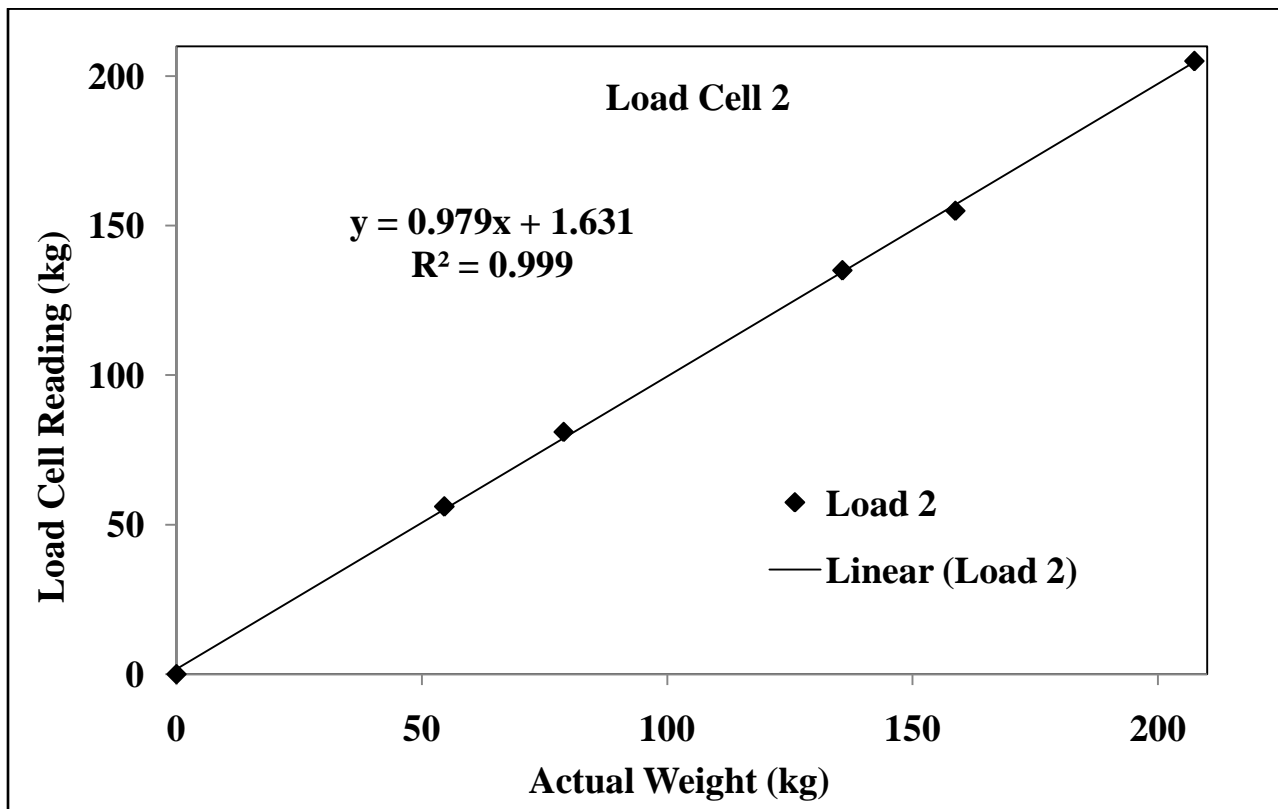


**Figure 3.5:** Calibration curve for load cell

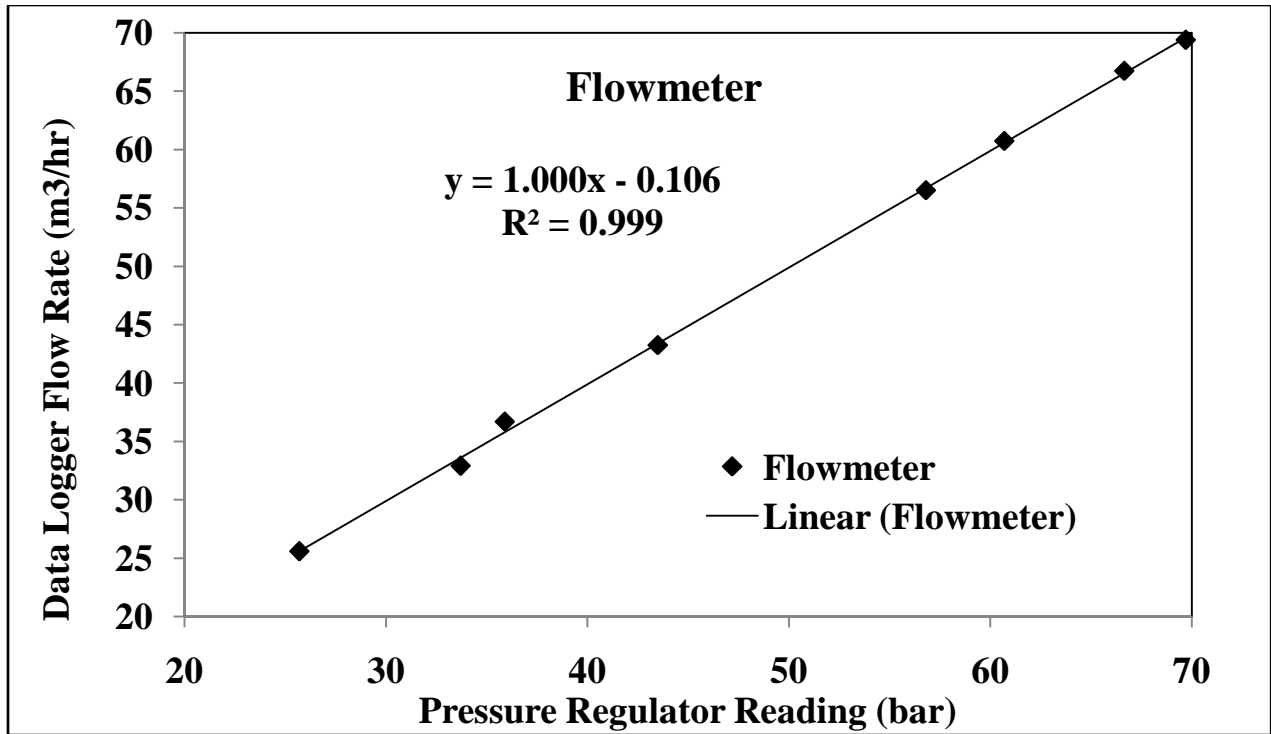


**Figure 3.6:** Calibration curve for flow meter

### 3.4 Operational Procedure

A standard operational procedure was used to perform the experiments over wide range of air and solid flow rates. Air flow rates were varied by changing the openings of globe valves installed in the pipeline, whereas solid mass flow rates were varied by changing the pre-pressurization of blow tank. There are two air lines in blow tank, one is top air line, which supplied the air for pre-pressurization of blow tank, other is fluidization air line, which was used to fluidize the material inside the blow tank and ensured that the materials would not stick to the walls of blow tank. Fluidization air line was also provided in receiver bin to prevent sticking of material.

The standard operational procedure to perform experiments is listed below;

- a) Air was allowed to reach the specified pressure in air storage tank by “TURN ON” the compressor and drier.
- b) After that, process air and instrumentation air supply was opened and set the pressure of process air to desired value using pressure regulator, whereas, set the pressure of instrumentation air to 5 bar (g).
- c) First, pneumatic panel and then PLC panel was switched ON followed by computer and it was ensured that data logger did the work properly.
- d) Before starting the experiments, calibration of all the pressure transducers, load cells and flow meter was done.
- e) Necessary settings of different globe valves were made and Cycle Start Button was pressed from PLC panel. At the same time Run Button in data logger should also be pressed.
- f) After that when the cycle was over, Stop Button in data logger was pressed and purging of the pipeline was done to clean it for next experiment.
- g) To repeat the procedure to perform further experiments, settings of globe valves was changed.

In each experiment, data logger recorded the readings of the load cell, flow meter and pressure transducer at certain intervals of the time. All these data points were plotted with respect to time and steady state conditions was found out where mass flow rate, pressure drop curves and slope of load cell showed good agreement. Pressure transients were taken up for selected range of steady state data to further investigation and found out the behaviour of pressure drop with respect to length, velocity and solid mass flow rate.

**CHAPTER 4: INVESTIGATION INTO PRESSURE  
FLUCTUATIONS**

#### 4.1 Conveying cycle signals

Figure 4.1 shows the typical pressure signal recorded during the pneumatic conveying cycle. As the cycle starts, material falls into the blow tank and is pre-pressurized to certain extent depending upon quantity of material. As the pressure in the blow tank becomes sufficient to push the material, conveying process starts and the solid-air mixture is conveyed through pipeline with steady state conditions. As the pipeline starts to get empty, pressure starts to drop and finally drops to zero.

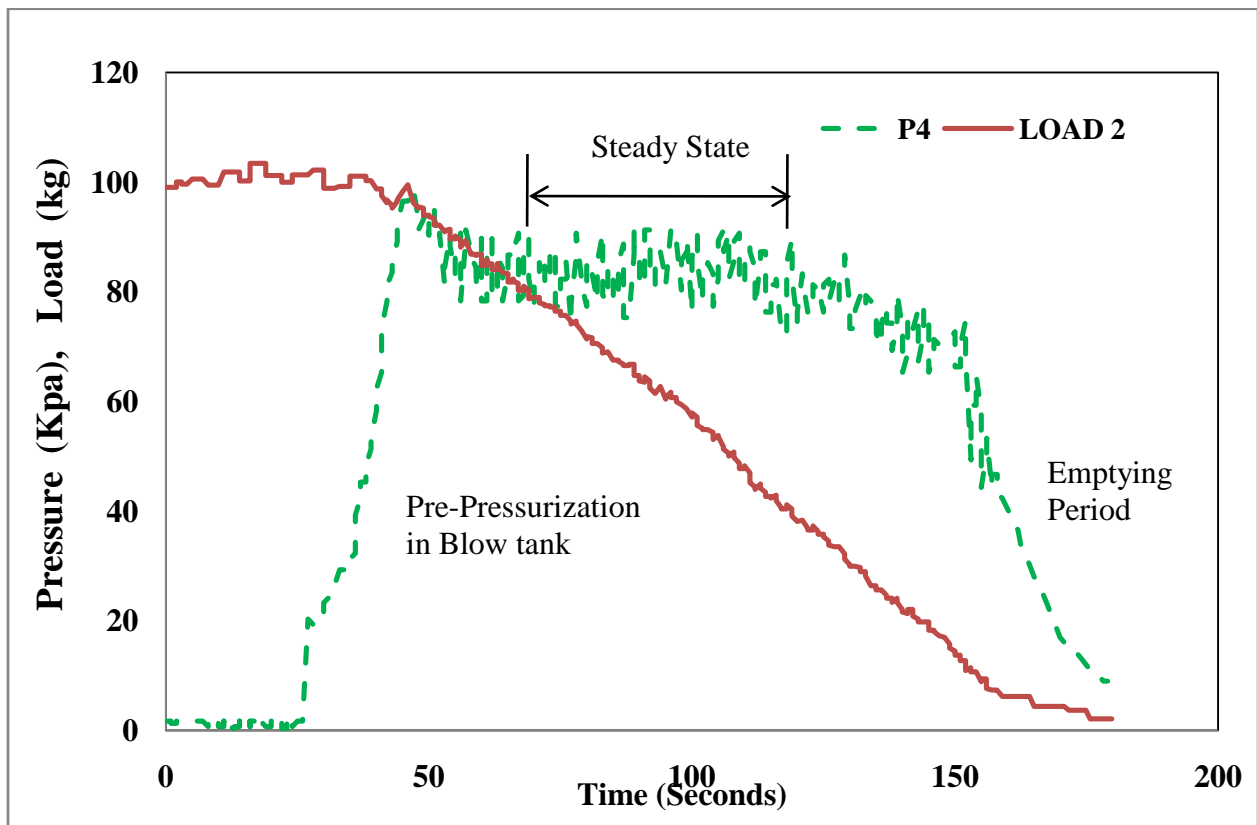
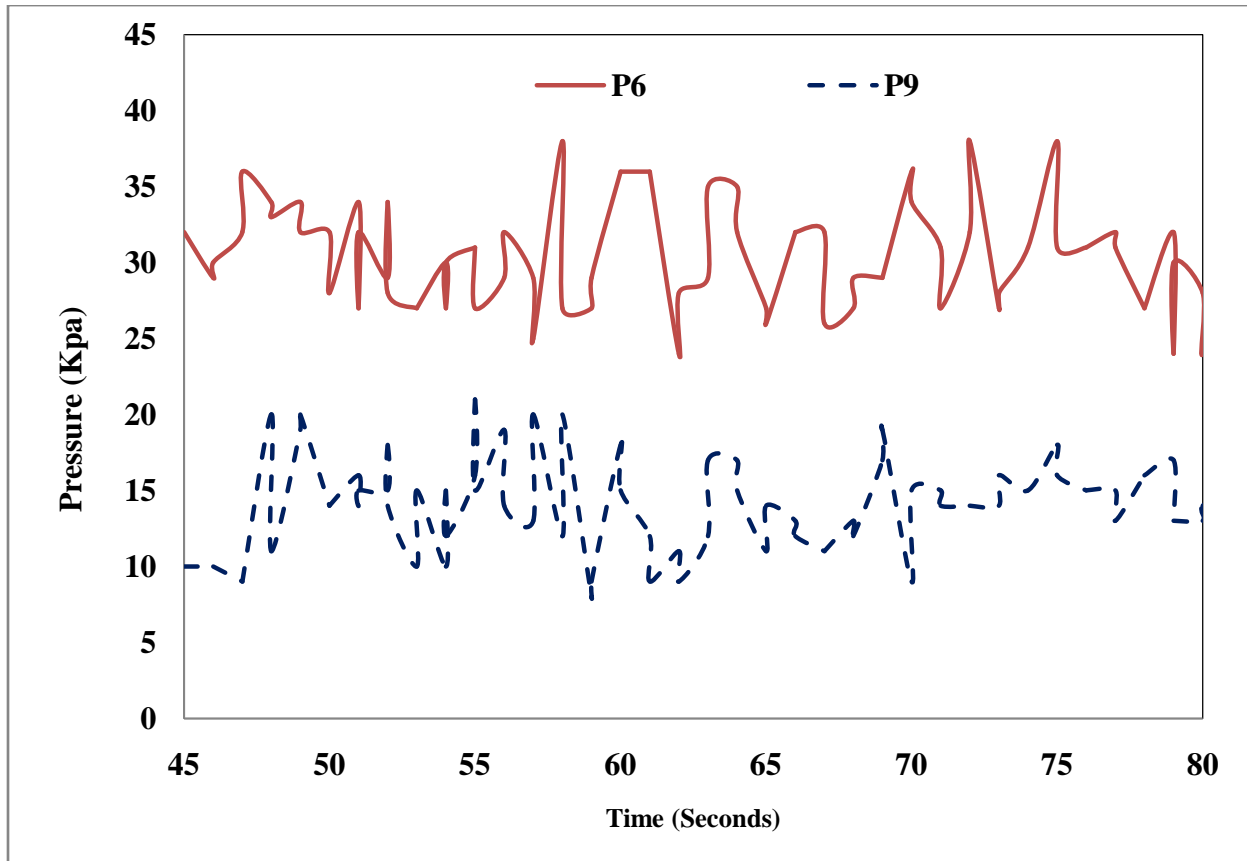


Figure 4.1: Signals obtained during conveying cycle

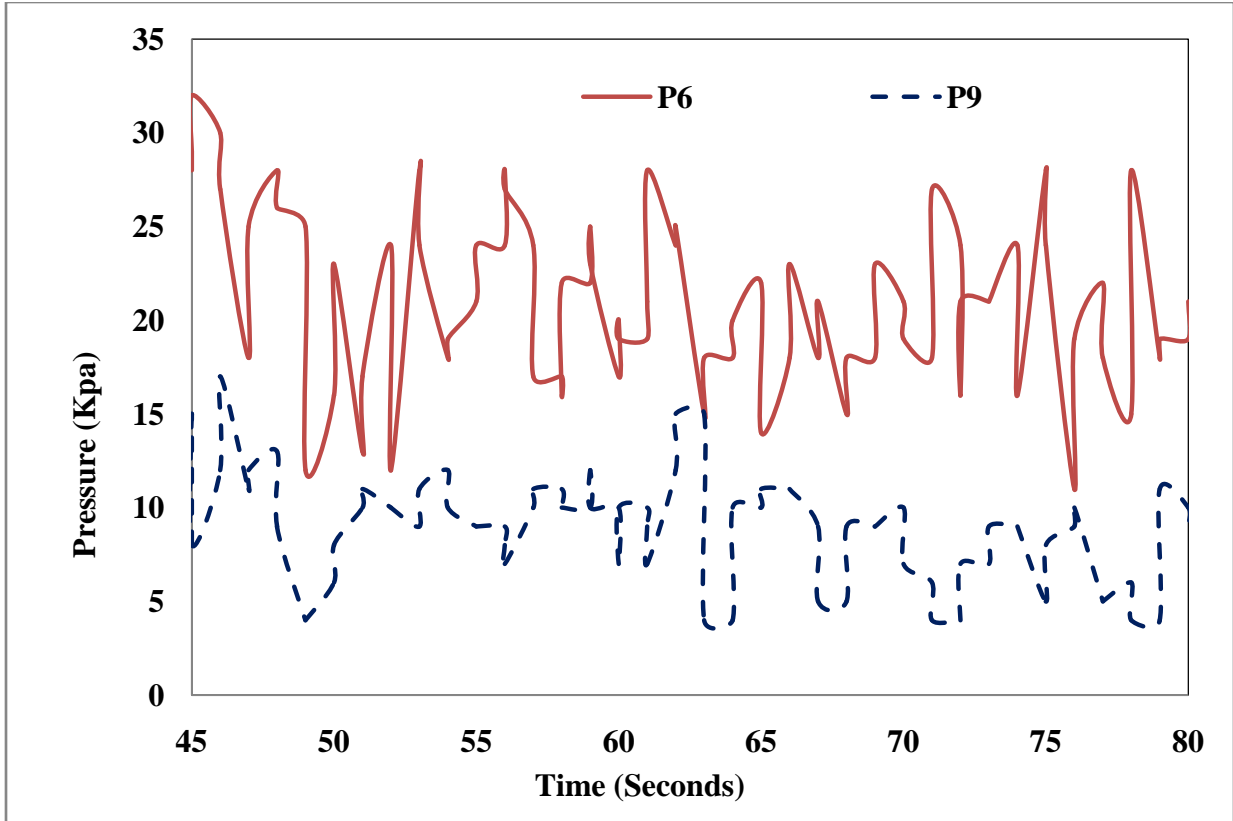
## 4.2 Pressure fluctuations

Figure 4.2 and 4.3 show typical pressure fluctuations versus time plots for fly ash being conveyed through 63 mm I.D. x 24 m long pipeline for different mass flow rates of air. Similarly, pressure fluctuations were obtained for another product for cement conveyed through 63 mm I.D. x 24 m long pipeline. Later both the products were conveyed through small diameter and longer pipeline (51 mm I.D. x 70 m long). Pressure fluctuations for pressure transducers P6 and P9 are shown in figures. In between P6 and P9, pressure transducers P7 and P8 are also there but their fluctuations are not shown in figures for clear visibility of pressure fluctuations.



**Figure 4.2:** Pressure Fluctuations (P6 & P9) for fly ash (63.5 mm I.D. x 24 m long pipeline)

$$(m_f = 0.052 \text{ kg/s}, \quad m_s = 4.2 \text{ t/hr})$$



**Figure 4.3:** Pressure Fluctuations (P6 & P9) for fly ash (63.5 mm I.D. x 24 m long Pipeline)

$$(m_f = 0.028 \text{ kg/s}, \quad m_s = 4.08 \text{ t/hr})$$

Figure 4.4 shows pressure fluctuations obtained from all pressure transducers (P6 to P9) for fly ash in 70 m long pipeline. It can be observed that pressure fluctuations have high value (average value 80 kPa for P6) compared to smaller length pipeline (24 m) for same  $m_f$  and  $m_s$  (shown in figure 4). Significant difference in pressure value for P7 and P8 pressure transducers can also be noticed because of large pressure drop in two bends coupled in pipeline between these pressure transducers. However, pressure fluctuations values are closer for straight pipe pressure transducers (P6 – P7) and (P8 – P9) which indicates that pressure drop is small in straight sections compared to bends.

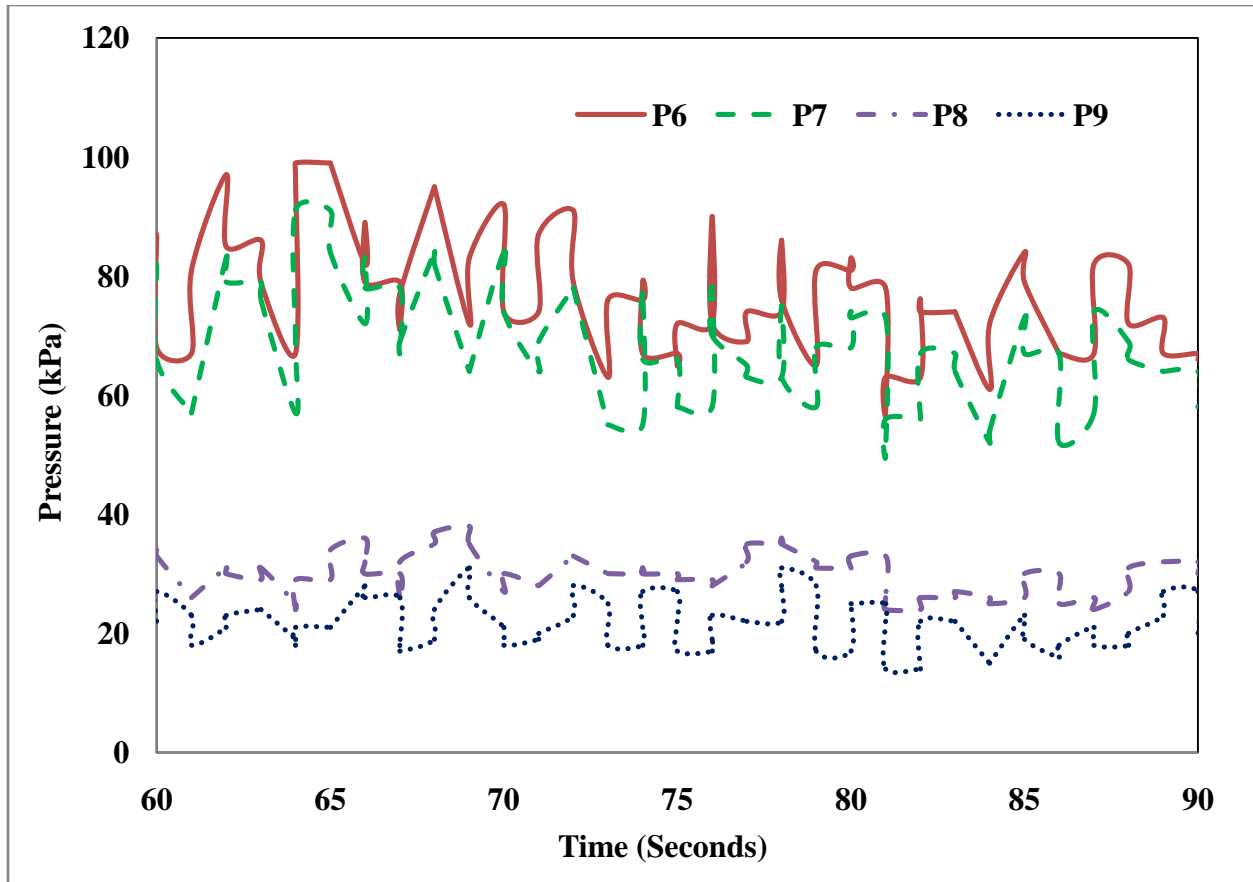


**Figure 4.4:** Pressure Fluctuations (P6 to P9) for fly ash (51 mm I.D. x 70 m long pipeline)

$$(m_f = 0.029 \text{ kg/s}, m_s = 4.4 \text{ t/hr})$$

Figure 4.5 shows pressure fluctuations obtained from all pressure transducers during conveying of cement in 63.5 mm I.D. x 24 m long pipeline. It can be seen that pressure fluctuations for cement has higher value (60 kPa for P6) compared to fly ash (35 kPa for P6) in same pipeline at the same mass flow rates (figure 4.2). It may be happen due to different behavior influenced by different particle properties shown by cement. At this mass flow rates, cement shows comparatively less transient behavior (less number of peaks compared to fly ash pressure fluctuations). However, cement show more random behavior at other mass flow rates (shown by A2.1)

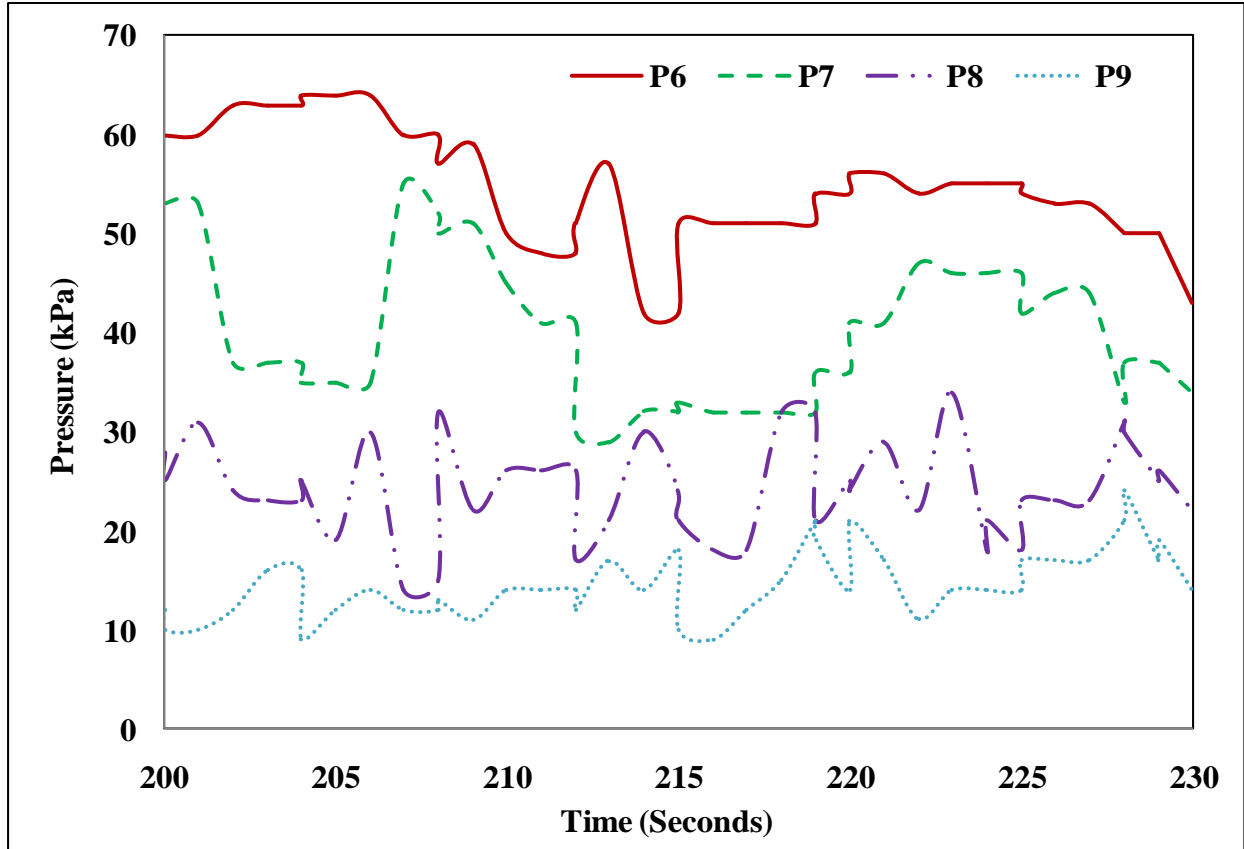


**Figure 4.5:** Pressure fluctuations (P6 to P9) for cement (63.5 mm I.D. x 24 m long pipeline)

$$(m_f = 0.05 \text{ kg/s}, m_s = 4.4 \text{ t/hr})$$

By observing of all figures, it appears that nature of signals obtained is different corresponding to different mass flow rates, different materials and different pipeline configurations. However to represent exact signal variation in terms of quantitative parameters to relate these with the change in flow mechanism requires certain signal processing methods. Shannon entropy technique has been used in this paper to investigate these pressure fluctuations and the effects contributed by operating parameters such as mass flow rate of air and solids. Steady state range of pressure signals were selected for 45 - 80 sec period for the purpose of analyzing pressure fluctuations.

### 4.3 Variation in Velocity and Density along the length of pipeline

Figure 4.6 shows the graph plotted between superficial air velocity difference and solid loading ratio for fly ash in 51 mm I.D. x 70 m long pipeline. Whereas, figure 4.7 shows the variation in density difference with respect to solid loading ratio for fly ash conveying in same pipeline. Difference of superficial air velocity and density is taken in between of two pressure tapping points P6 (close to inlet of pipeline) and P9 (close to exit of pipeline). From figure 4.6, it can be seen that difference in superficial air velocity reduces with increase in solid loading ratio. Higher difference in superficial air velocity at low solid loading ratio indicates that velocity increases significantly from the inlet to the exit of pipeline compared to high solid loading ratio where small increase in the superficial air velocity takes place.

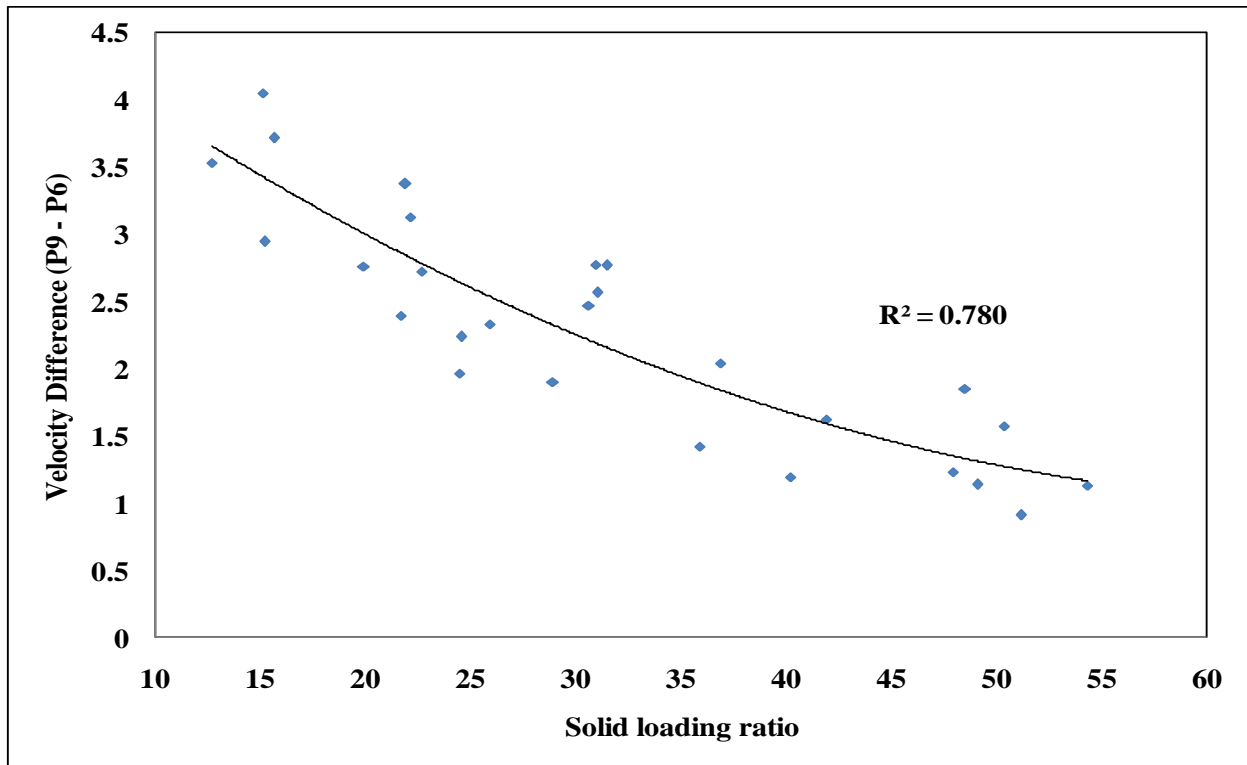


**Figure 4.6:** Velocity difference versus solid loading ratio for fly ash  
(51 mm I.D. x 70 m long pipeline)

From figure 4.7, it can be observed that difference in density increases with increase in solid loading ratio. Density of material reduces along the length of pipeline from the inlet of pipeline to the exit of pipeline. It indicates that as flow approaches towards the end of pipeline, material density decreases at cross section of pipeline with increase in superficial air velocity. Higher value of density difference is obtained at higher solid loading ratio and lower value of density difference is obtained at lower solid loading ratio. Lower solid loading ratio indicates the higher value of air mass flow rate ( $m_f$ ) and corresponding higher superficial air velocity compared to solid mass flow rate ( $m_s$ ). Velocity difference between exit of pipe and inlet of pipe is also higher at lower solid loading ratio shown by figure 4.6. it can be interpreted that higher velocity at inlet of pipeline remain higher at exit of pipeline without significant change in density of material or dilute phase at inlet remain dilute at exit of pipeline also. But at higher solid loading ratio (mean low value of superficial air velocity), change in density occurs significantly with small increase in superficial air velocity. This phenomenon interprets that dense phase at beginning of pipeline could be converted into dilute phase at end of pipeline for higher solid loading ratio.

In case of 63.5 mm I.D x 24 m long pipeline, very small change in superficial air velocity is found out even for low mass solid loading ratio. That's why; graphs for that pipeline are not plotted here. It may be happen due to small length of pipeline (24 m) which is not sufficient for expansion of air on changing flow pattern and flow conditions along the length of pipeline influenced by other parameters like solid loading ratio.

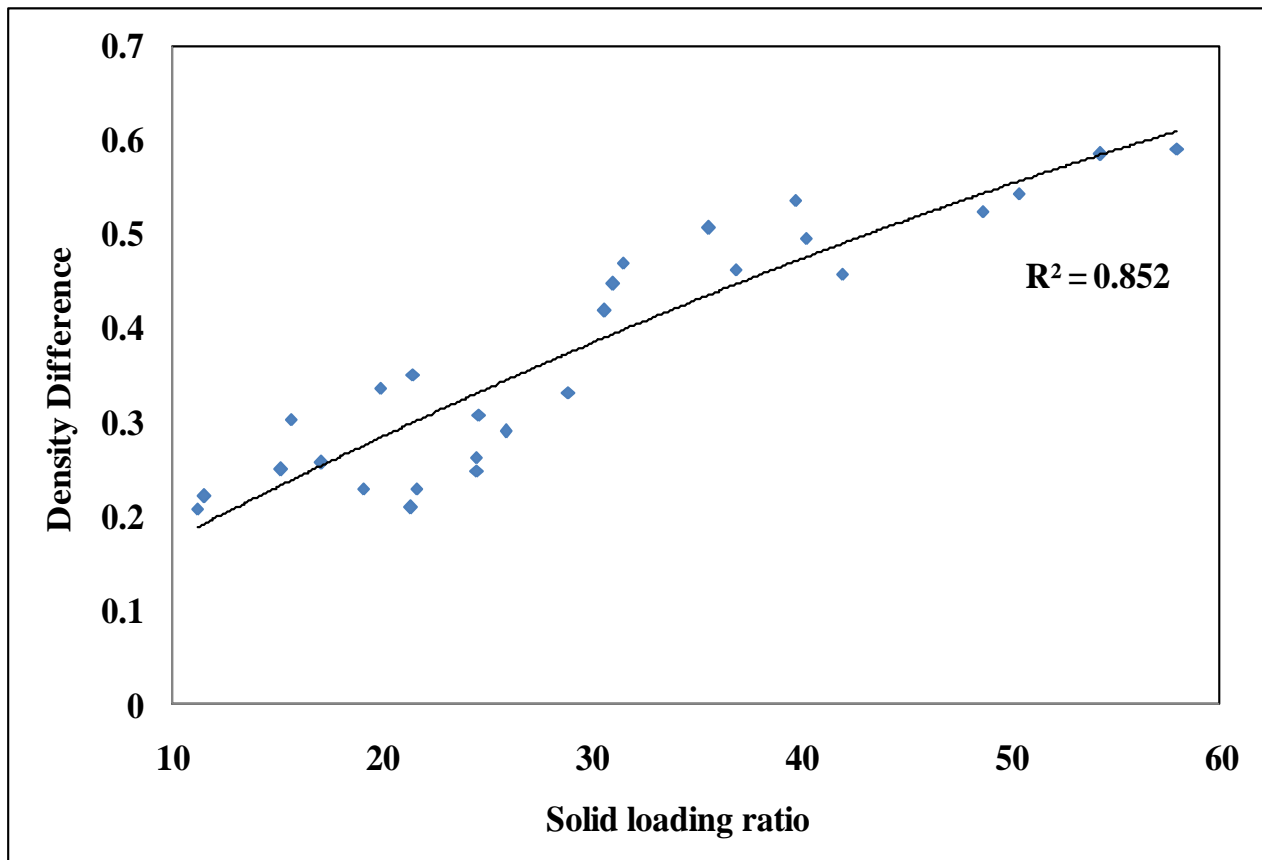


**Figure 4.7:** Density difference versus solid loading ratio for fly ash  
(51 mm I.D. x 70 m long pipeline)

## **CHAPTER 5: RESULTS AND DISCUSSION**

This chapter presents the result of investigation being done on transient pressure fluctuations using Shannon entropy and standard deviation method. Shannon entropy technique is chosen because of its ability to analyze the peculiar or transient features of pressure fluctuations and to extract information about flow conditions. Some brief introduction about Shannon entropy is also given initially in this chapter. All the results present in form of different type of graphs to observe the variations of Shannon entropy with various parameters such as length, solid loading ratio and superficial air velocity covering all experiments and range of values with probable reason behind occurrence of these variations.

## 5.1. Shannon Entropy

Shannon entropy is the measurement of amount of information and degree of indeterminacy in certain system (Shannon, 1948). It can be utilized to predict the degree of uncertainty involved in predicting the output of probabilistic event. Shannon entropy of pressure time series in pneumatic conveying can be calculated as:

$$S = -\sum_{i=1}^N P(X_i) \log_b P(X_i) \quad (4)$$

Where, N is the number of possible states for a given time series  $\{X_1, X_2 \dots X_N\}$  each one with its probability  $P(X_i)$  (No. of values in selected discrete data set  $(X_i)$  divided by total number of possible states, N). When  $b = 2, e$  and  $10$ , the unit of S is a bit, nat and hart, respectively. If one event  $(X_i)$  has probability of one and all other probabilities are zero, Shannon entropy has minimum value. On the contrary, if events are equally probable, largest entropy is obtained.

In this study, Shannon entropy values are calculated by using base value 2. Figures 5.1 and 5.2 present the changes in Shannon entropy along the length of pipeline for fly ash for two different pipelines. Figures 5.3 and 5.4 reveal Shannon entropy variation for cement for the same pipelines as for the fly ash. Figures consist of various trend lines indicating different experiments conducted with different set of solid mass flow rate and air mass flow rate.

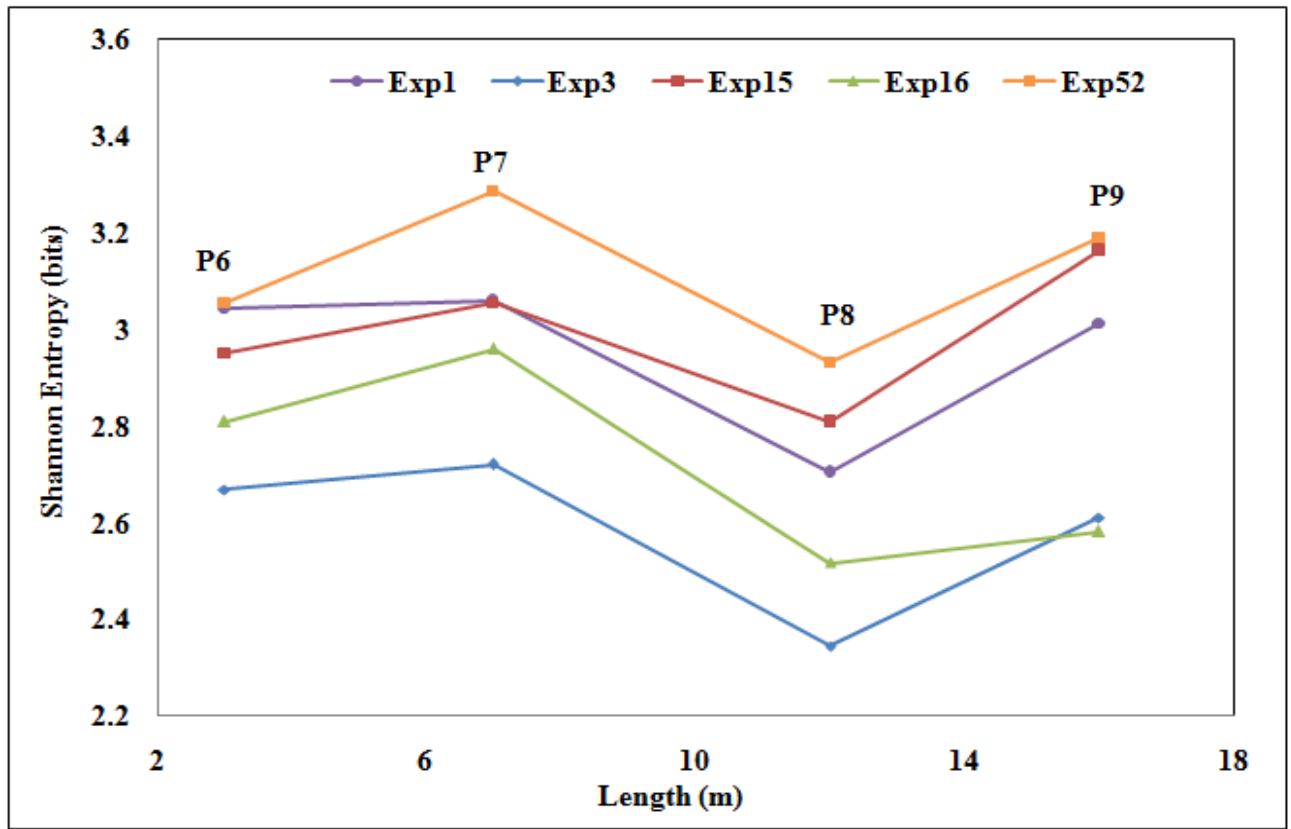


**Figure 5.1:** Shannon Entropy versus pipeline length for fly ash

(63 mm I.D. x 24 m long pipeline)

( $m_f = 0.025 - 0.05$  kg/s;  $m_s = 4 - 6$  t/hr)

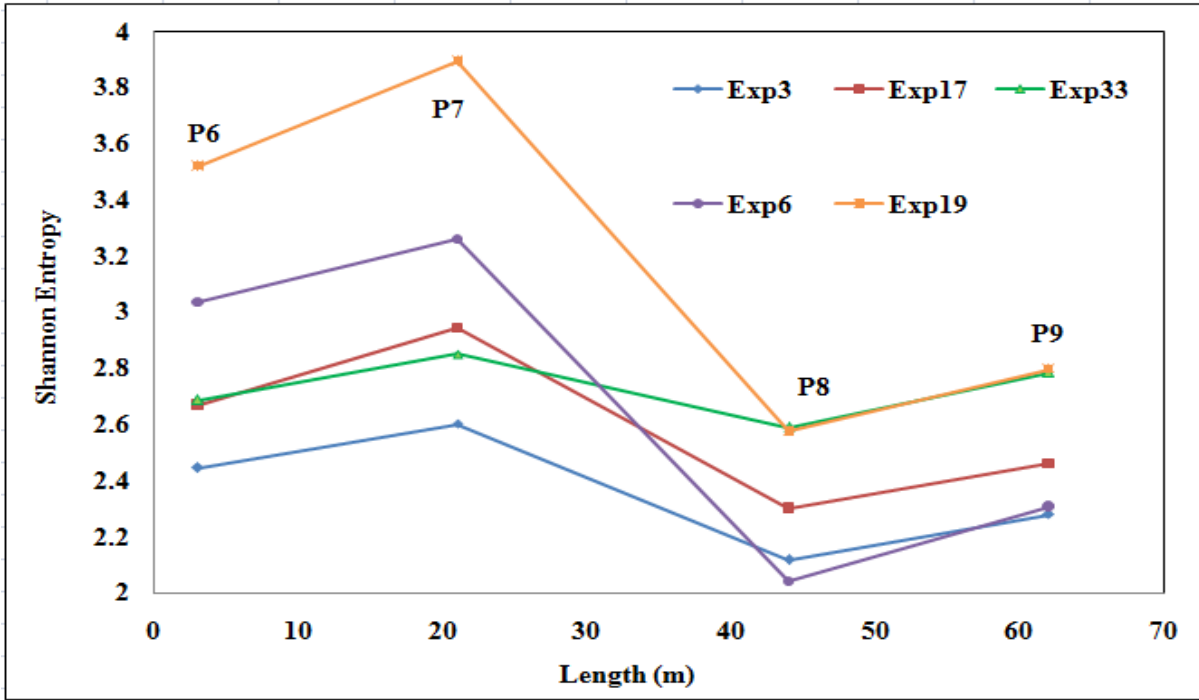


**Figure 5.2:** Shannon Entropy versus pipeline length for fly ash (51 mm I.D. x 70 m long pipeline)  
 ( $m_f = 0.016 - 0.039$  kg/s;  $m_s = 2 - 4$  t/hr)

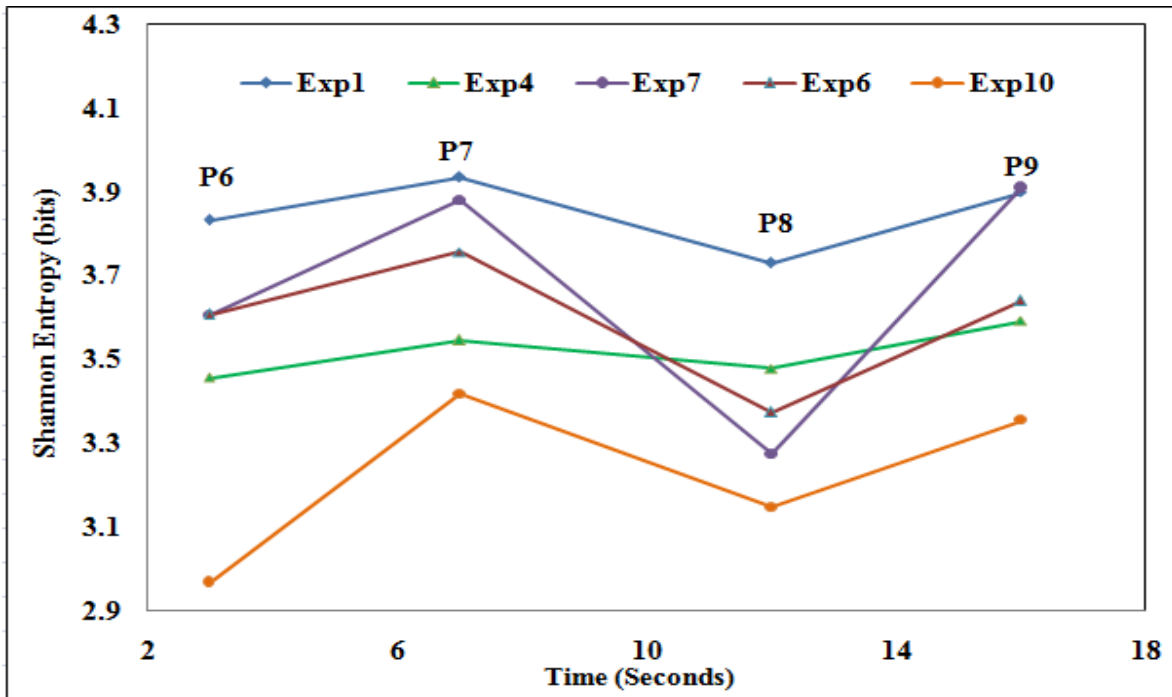


**Figure 5.3:** Shannon Entropy versus pipeline length for Cement (63 mm I.D. x 24 m long pipeline)  
 ( $m_f = 0.015 - 0.038$  kg/s;  $m_s = 4 - 7$  t/hr)

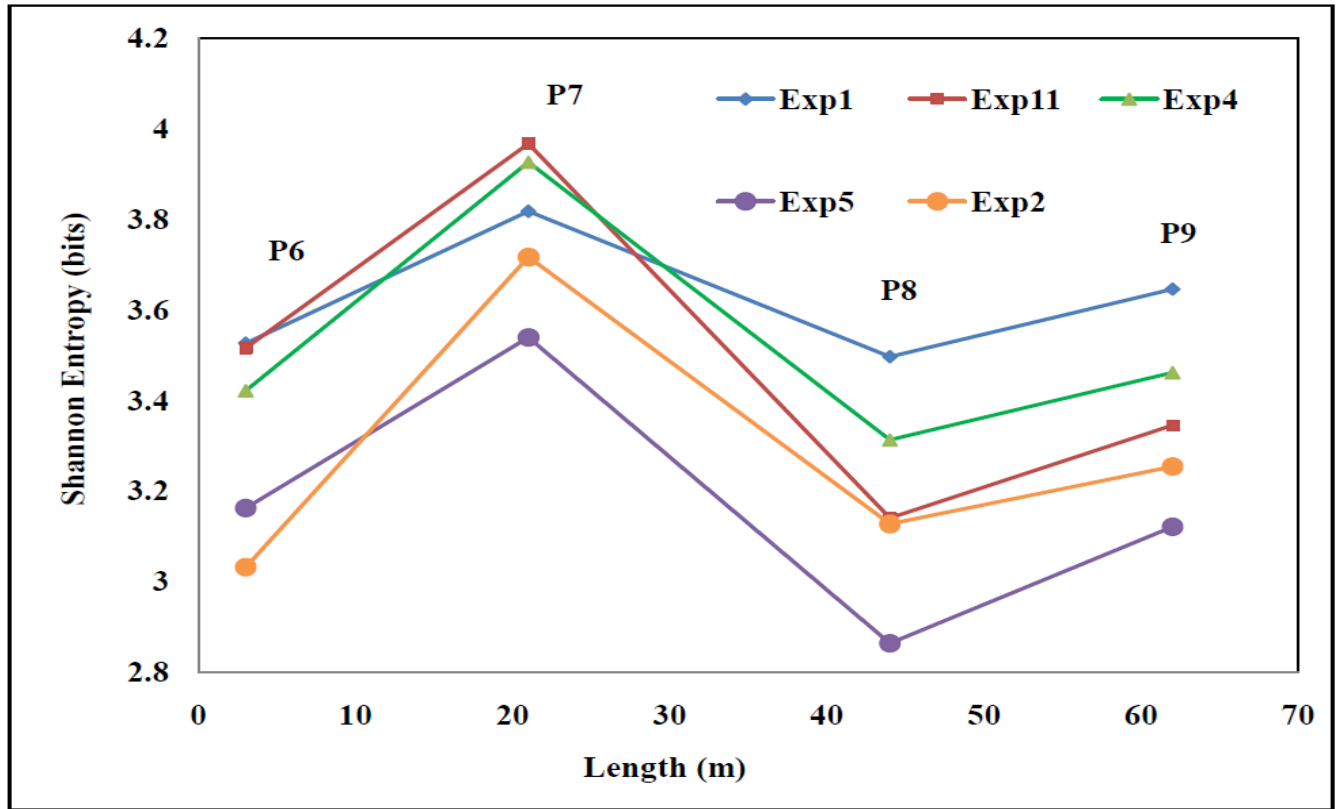


**Figure 5.4:** Shannon Entropy versus pipeline length for Cement

(51 mm I.D. x 70m long pipeline)

( $m_f = 0.026 - 0.050$  kg/s;  $m_s = 2 - 3$  t/hr)

It can be seen that Shannon entropy value increases along the flow direction for straight pipe section (P6 to P7). However, there is decrease in value of Shannon entropy during flow through the bend (P7 to P8). Two bends ( $90^\circ$  with 1 m radius of curvature) were coupled between P7 to P8. Increasing value of Shannon entropy indicates that the randomness of pressure fluctuations is increasing along the flow direction through the straight pipe sections. The possible cause for this phenomenon could be carrier gas expansion (due to pressure drop) in constant diameter pipeline and increase in turbulence effect related with increasing air velocity. The reason for fall in value

of Shannon entropy across the bend could be deceleration of particles while passing through bend and reduction in the air flow turbulence across the bend (Mittal, 2015). For straight section P8 to P9 after bend, rise in value of Shannon entropy takes place and gives slight increase in overall value of Shannon entropy in case of 63 mm I.D. x 24 m longer pipeline in certain experiments while in some of the experiments, there was no change observed in the overall value of Shannon entropy. For another pipeline of 51 mm I.D. x 70 m length, overall decrease was found in value of Shannon entropy for both the products (i.e. fly ash and cement) due to large drop in value across the bend (because of the two 90<sup>0</sup> degree bend coupled in between two pressure transducers P7 and P8) as compared to increase found in straight pipe sections and not adequate straight pipe length in the downstream section of bend to regain the momentum loss of particles. Flow through bend is very complex phenomenon and difficult to understand. Drop in value may be due to unique surface characteristics of fine powders which made it sticky to pipe wall and cause reduction in velocity of particles (Venkatasubramanian, 2000). Besides, rise in temperature due to impact of high velocity (due to additional expansion of gas in increased length of pipeline in 70 m pipeline compared to 24 m long pipeline before bend) particles favored this process. Though, various changes can be noticed from graphs but it is not sufficient to conclude about change in flow pattern along the pipeline because of insignificant change in length of pipeline and total length of pipeline is short. But, increasing value of Shannon entropy along the straight pipe section indicates increase in degree of complexity and disorder of flow pattern. For the longer pipelines, as the length increases, phase of flow changes itself along the length from the inlet of pipe to exit of pipe. Similar trend can be perceived for Shannon entropy along the length of pipeline in case of cement. However, few experiments has not shown same trend in all cases. Comparison of figures 5.1 and 5.2 reports the difference in value of Shannon

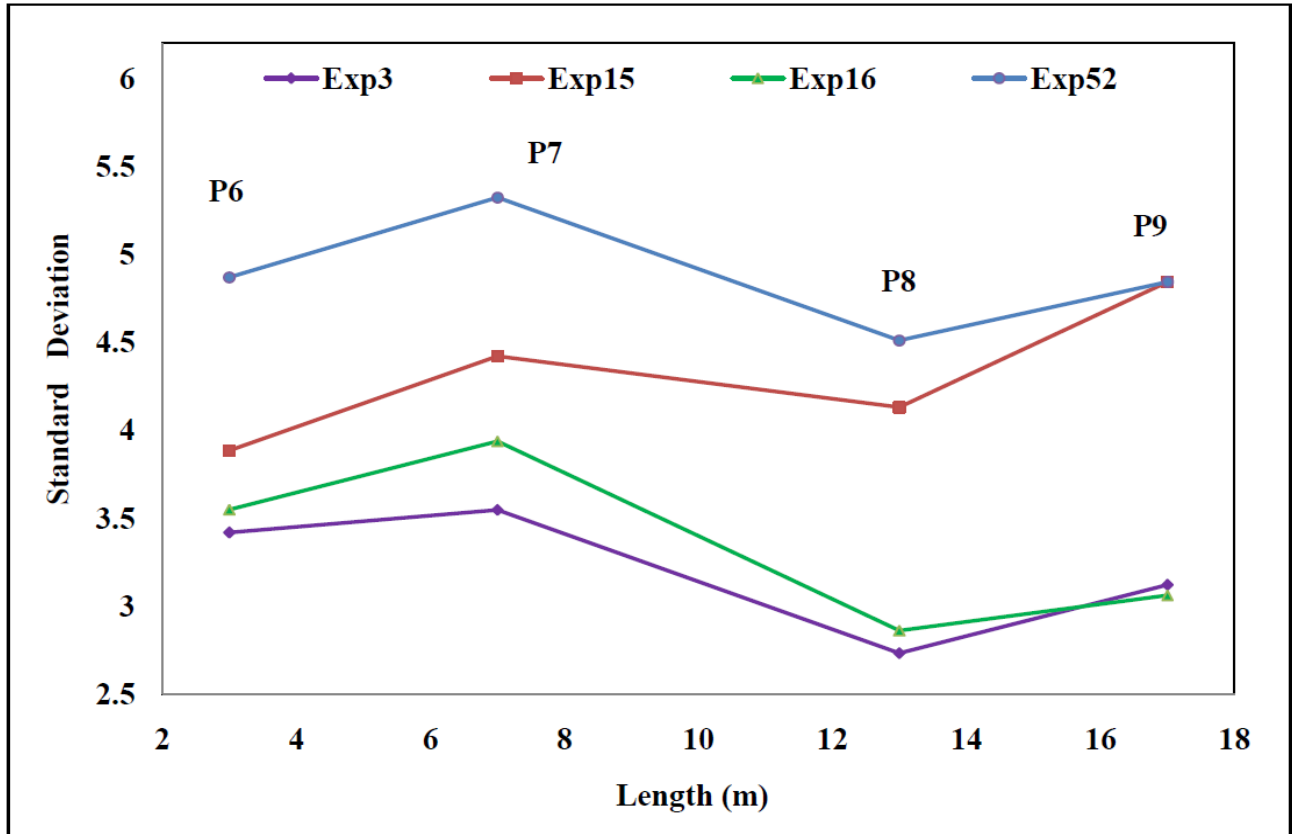
entropy between both pipelines caused by the changes in configuration of pipe (length and diameter). Experiments for fly ash in 51 mm I.D. x 70 m long pipeline have more range of Shannon entropy value than the experiments (having same range of value of  $m_f$  and  $m_s$ ) for fly ash in 63 mm I.D. x 24 m long pipeline due to increasing value of friction factor and corresponding pressure drop. It indicates that changes in pipeline configuration parameters (i.e. decrease in diameter and increase in length of pipeline) have an effect on pressure fluctuations.

Comparison of entropy values of fly ash and cement (Figure 5.1 and 5.3) show that range of Shannon entropy values for cement (3 – 4 bits) is more as compared to fly ash (2.3 to 3.3 bits) for 63 mm I.D. x 24 m long pipeline for same range of  $m_f$  and  $m_s$  caused by different bulk material properties of cement from fly ash. Cohesive nature of cement due to smaller particle diameter and higher particle density makes it little difficult to transport at very low velocities which is characterized by enhanced pressure fluctuations.

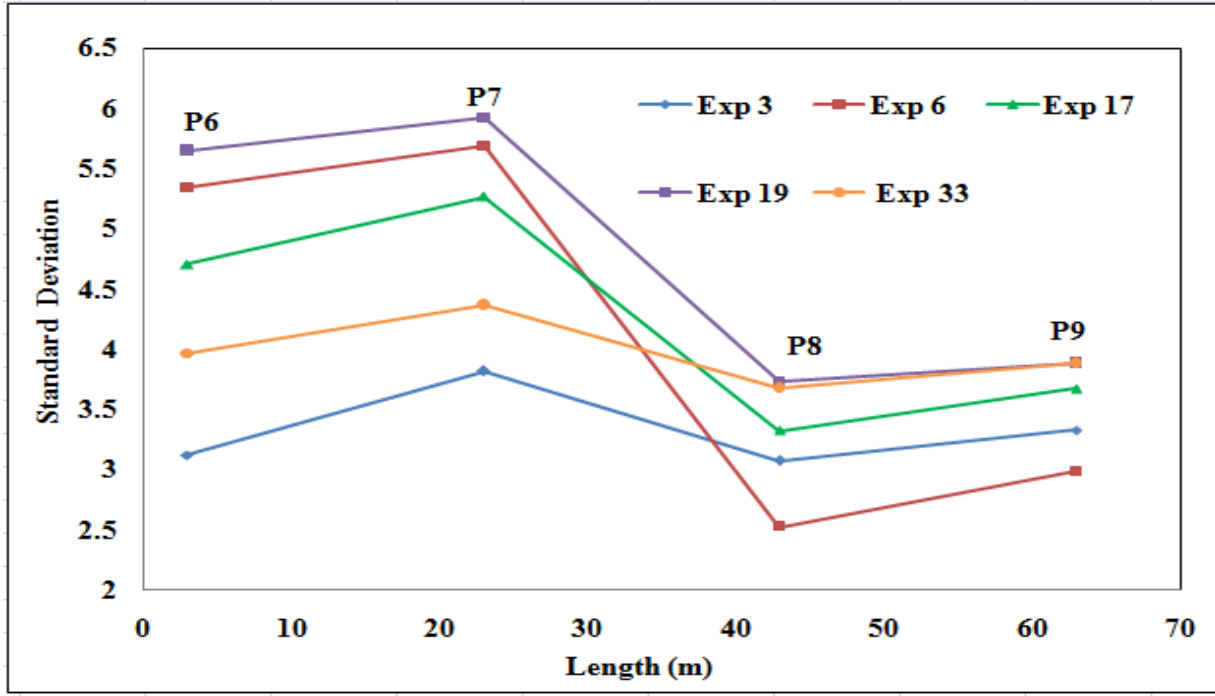
## **5.2. Standard deviation**

Figure 5.5 and 5.6 illustrate standard deviation plots for fly ash in different pipelines while figures 5.7 and 5.8 illustrate standard deviation plots for cement in same pipelines. Deviation from its mean value represents the fluctuations in the signal, therefore larger values of standard deviation, indicate towards higher fluctuations in the signal. Variations in standard deviation are similar to variations in Shannon entropy along the length of pipeline indicate that both techniques sense the same type of behavior of flow pattern. Large values of standard deviation is observed in case of cement compared to standard deviation values of fly ash by comparison of figure 5.5 and 5.6. It indicates that cement shows more chaotic behavior of flow pattern.

However, longer pipeline in case of cement does not show same behavior (value of standard deviation decreased with increase in length of pipeline) as in case of fly ash (value of standard deviation increased).



**Figure 5.5:** Standard deviation versus pipeline length for fly ash  
 (63 mm I.D. x 24 m long pipeline)  
 ( $m_f = 0.025 - 0.05$  kg/s;  $m_s = 4 - 6$  t/hr)



**Figure 5.6:** Standard deviation versus pipeline length for fly ash (51 mm I.D. x 70 m long pipeline)

( $m_f = 0.016 - 0.039$  kg/s;  $m_s = 2 - 4$  t/hr)

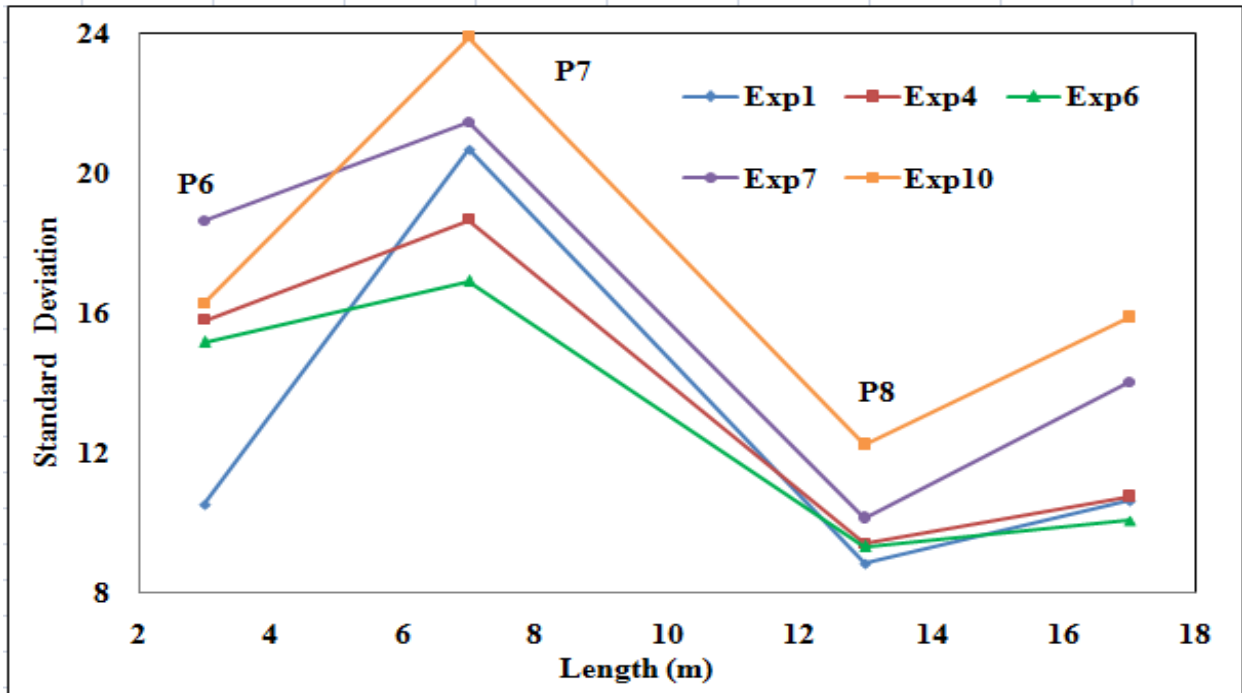


**Figure 5.7:** Standard deviation versus pipeline length for cement (63 mm I.D. x 24 m long pipeline)

( $m_f = 0.015 - 0.038$  kg/s;  $m_s = 4 - 7$  t/hr)

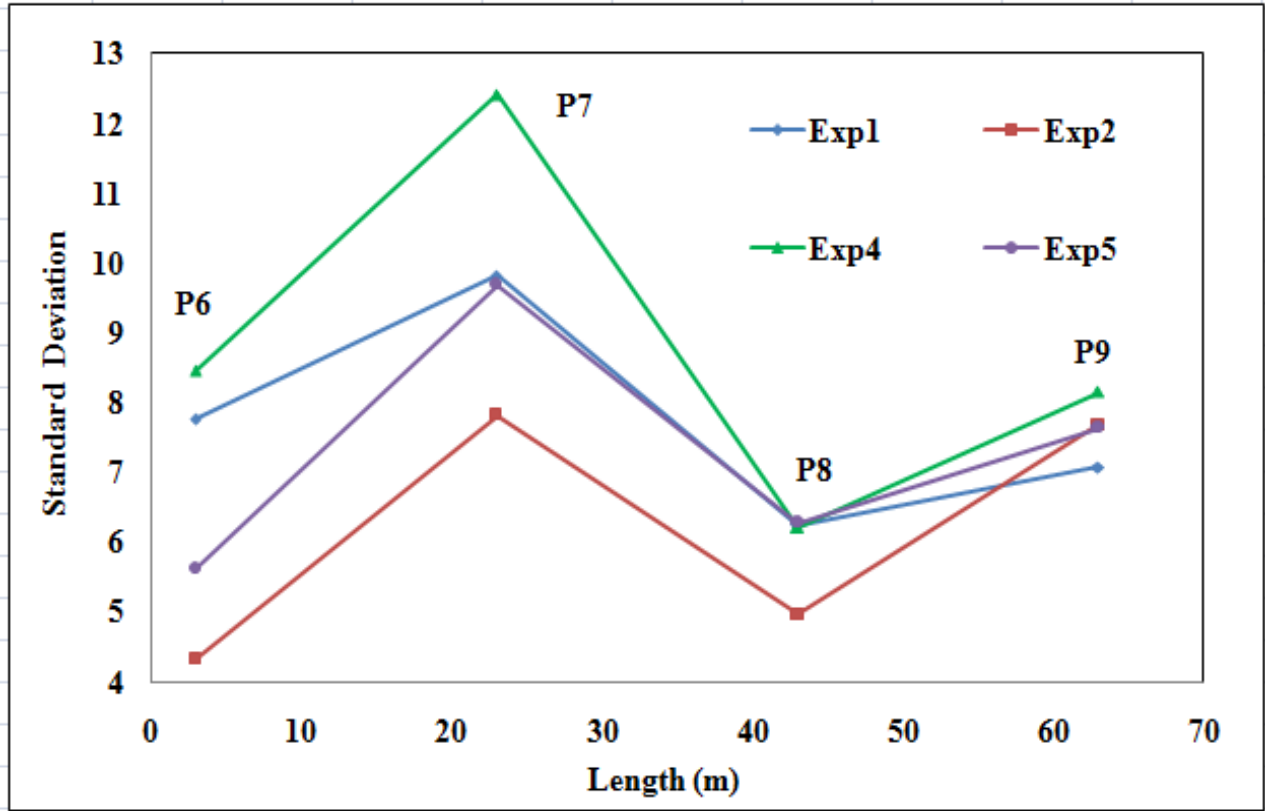


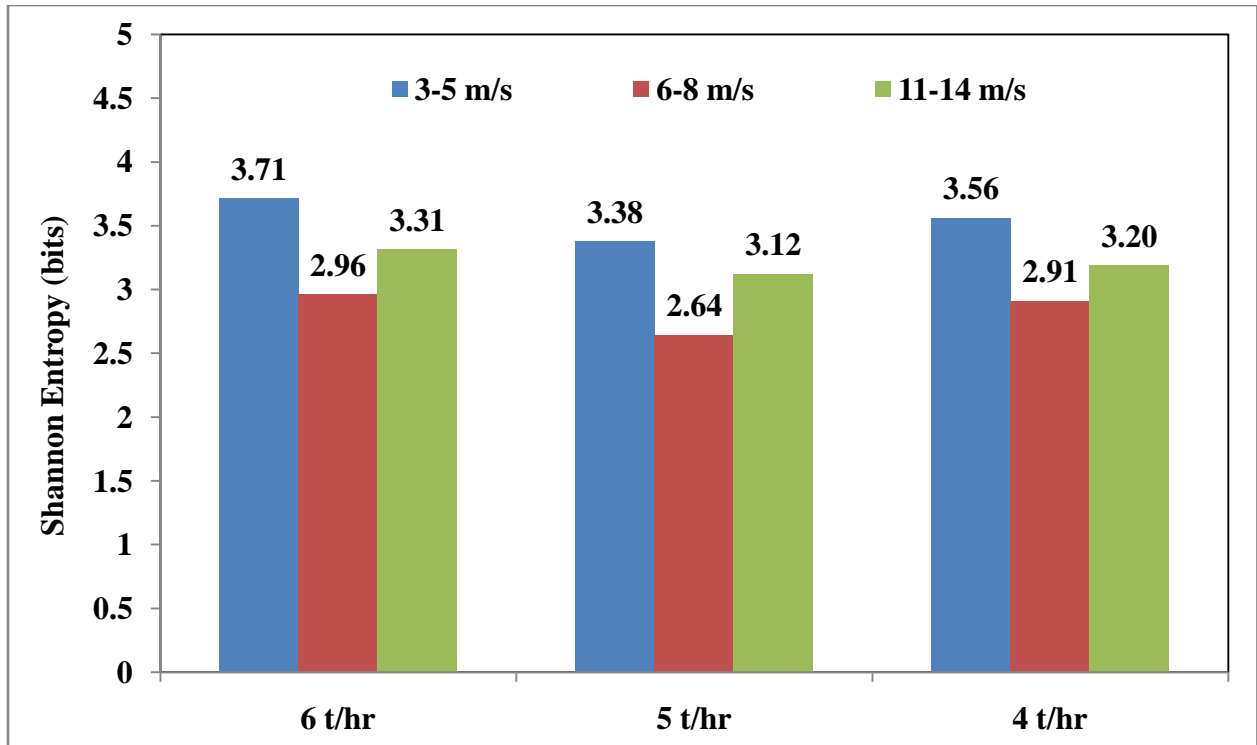
**Figure 5.8:** Standard deviation versus pipeline length for cement (51 mm I.D. x 70 m long pipeline)  
 ( $m_f = 0.026 - 0.050$  kg/s;  $m_s = 2 - 3$  t/hr)

### 5.3 Effect of superficial air velocity

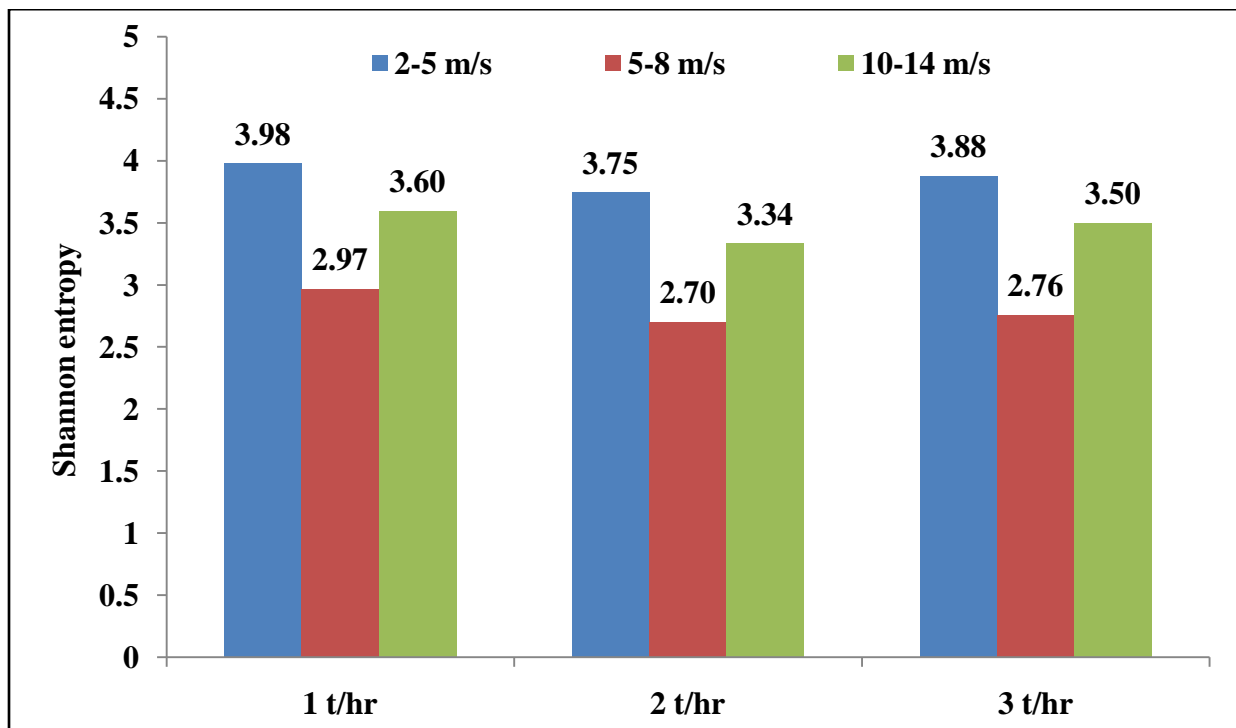
Figure 5.9 and 5.10 show the values of Shannon entropy at a particular pressure transducer location for different velocities for fly ash and cement. Both figures consist of three data sets corresponding to different set of values of solid mass flow rate. It is noticeable that at low velocities (3-5 m/s), values of Shannon entropy is high (3.3 to 3.7) compared to medium velocities (6-7 m/s) and high velocities (11-14 m/s). Least values of Shannon entropy (2.6 to 3.0) is obtained for medium velocities while for high velocities, value of Shannon entropy lies

between value of low and medium velocities. At very low velocity, gas-solid mixture flows in dense phase in which particles tend to deposit at bottom of pipe and formation of unsteady dunes. It makes system unstable and produces sudden rise in pressure fluctuations with reducing velocity. At medium superficial air velocities, Shannon entropy value decreases because the flow tends to stabilize in the conveying pipeline and approaches to steady state conveying condition with reduction in pressure fluctuations. However, for higher superficial air velocities, random interactions (between particle and air) are enhanced, indicated by high value of Shannon entropy relative to the value at medium velocities but less than the value at low velocities. The reason for small change in the value of Shannon entropy at high velocities compared to large change in value of Shannon entropy at low velocities could be that superficial air velocity has little effect on flow characteristics at higher velocities compared to low velocities. At low velocities, little change in velocity significantly affects the flow pattern and its characteristics.

Similar trend can be seen for cement in 63 mm I.D. x 24 m long pipeline and found that values of Shannon entropy is little high for cement (3.7 - 4.0) compared to fly ash (3.3 - 3.7) in 63 mm I.D. x 24 mm long pipeline at low velocities which could be due to unstable dune formation in case of cement caused by its small diameter (15 $\mu$ m) and particle density compared to fly ash (45 $\mu$ m). Conveying in the low velocities region indicates dense phase, material transports through pipe with filled cross section in form of unstable long plug in case of small particles which can leads to blockage. So, High value of Shannon entropy (corresponding to minimum conveying velocity) can be acted as a precursor of blockage of pipe.

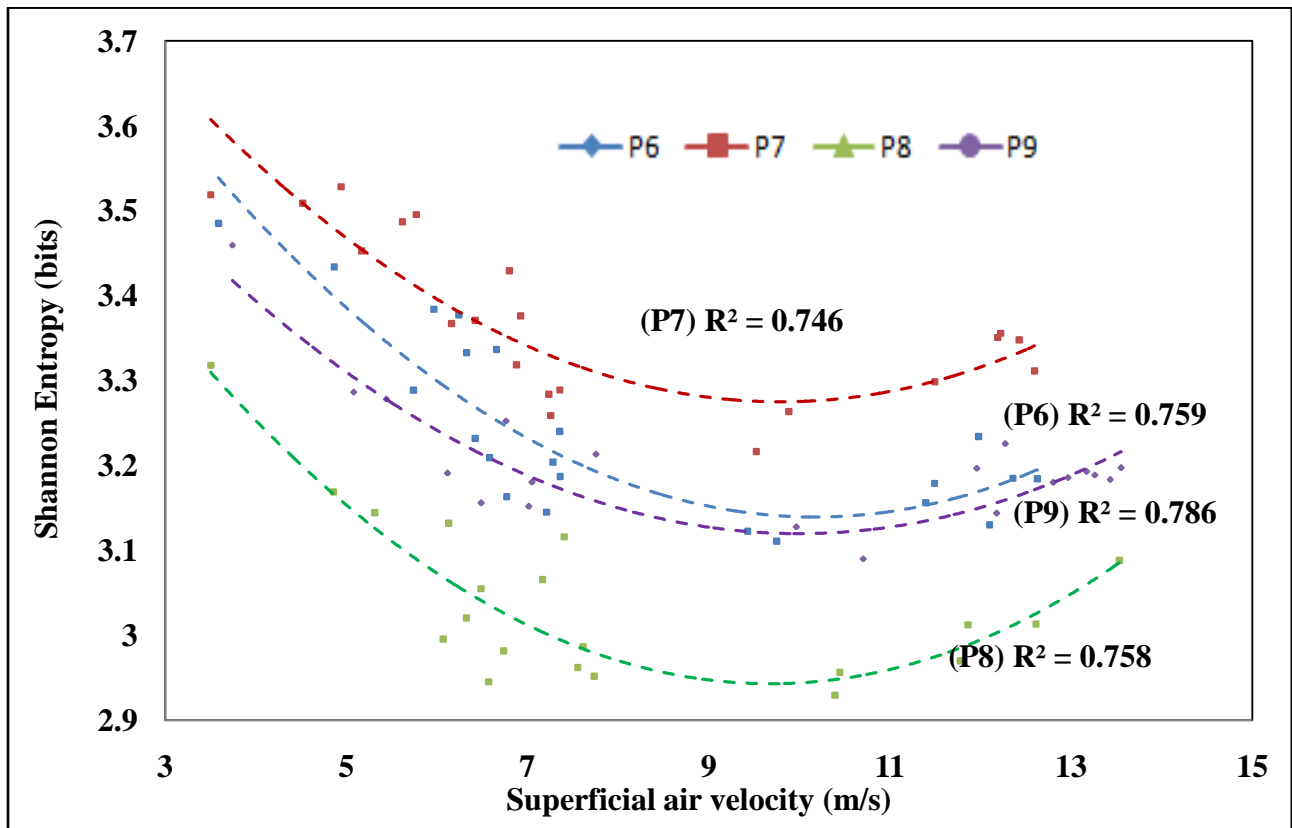


**Figure 5.9:** Shannon Entropy for fly ash at different velocity ranges (63 mm I.D. x 24 m long pipeline)



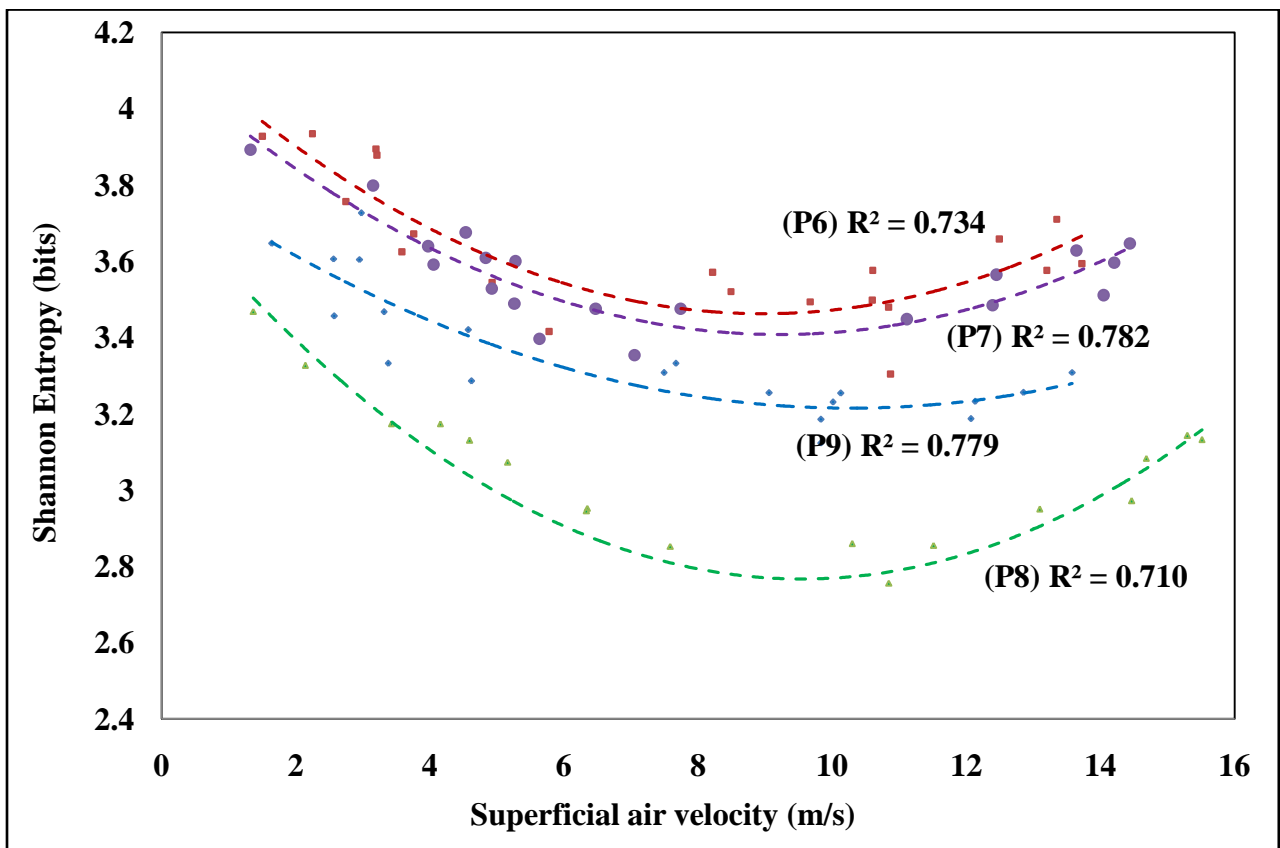
**Figure 5.10:** Shannon entropy for cement at different velocity ranges (63 mm I.D. x 24 m long pipeline)

Figure 5.11 and 5.12 show the variation in Shannon entropy for all pressure transducers with respect to superficial air velocity covering all experiments from dense to dilute phase pneumatic conveying. Figure 5.13 shows variations for fly ash product while figure 5.14 shows variations for cement test product. Same result can be observed by these figures as given by above figures with continuous variation in Shannon entropy with respect to all values of superficial air velocity. Values of Shannon entropy is higher for low velocities (less than 5 m/s for fly ash and less than 3 m/s for cement). Sharp rise in Shannon entropy can be seen as velocities decreases beyond the corresponding minimum conveying velocity and higher values can be noticed in case of cement at low velocities. Value of R2 is only 70-75 %, which is not very high. Dashed lines are tentative trends. Hence further work is required.



**Figure 5.11:** Shannon entropy versus superficial air velocity for fly ash (63.5 mm I.D. x 24 m long pipeline)

At mid velocities region (6 to 9 m/s), slowly rise in value of Shannon entropy with decrease in velocities can be observed as a transition from dilute phase to dense phase. The point from which value of Shannon entropy tends to increase towards low velocities region can be identified as point of minimum pressure drop. Subsequent to that pressure drop due to particle or solid phase contribute more in total pressure drop than pressure drop due to air only and makes system enter into unstable boundary.



**Figure 5.12:** Shannon entropy versus superficial air velocity for cement

(63.5 mm I.D. x 24 m long pipeline)

#### 5.4. Effect of solid mass flow rate

Figures 5.13 to 5.14 show the variation of Shannon entropy versus length at constant  $m_f$  to know the effect of solid mass flow rate ( $m_s$ ) on flow characteristics.

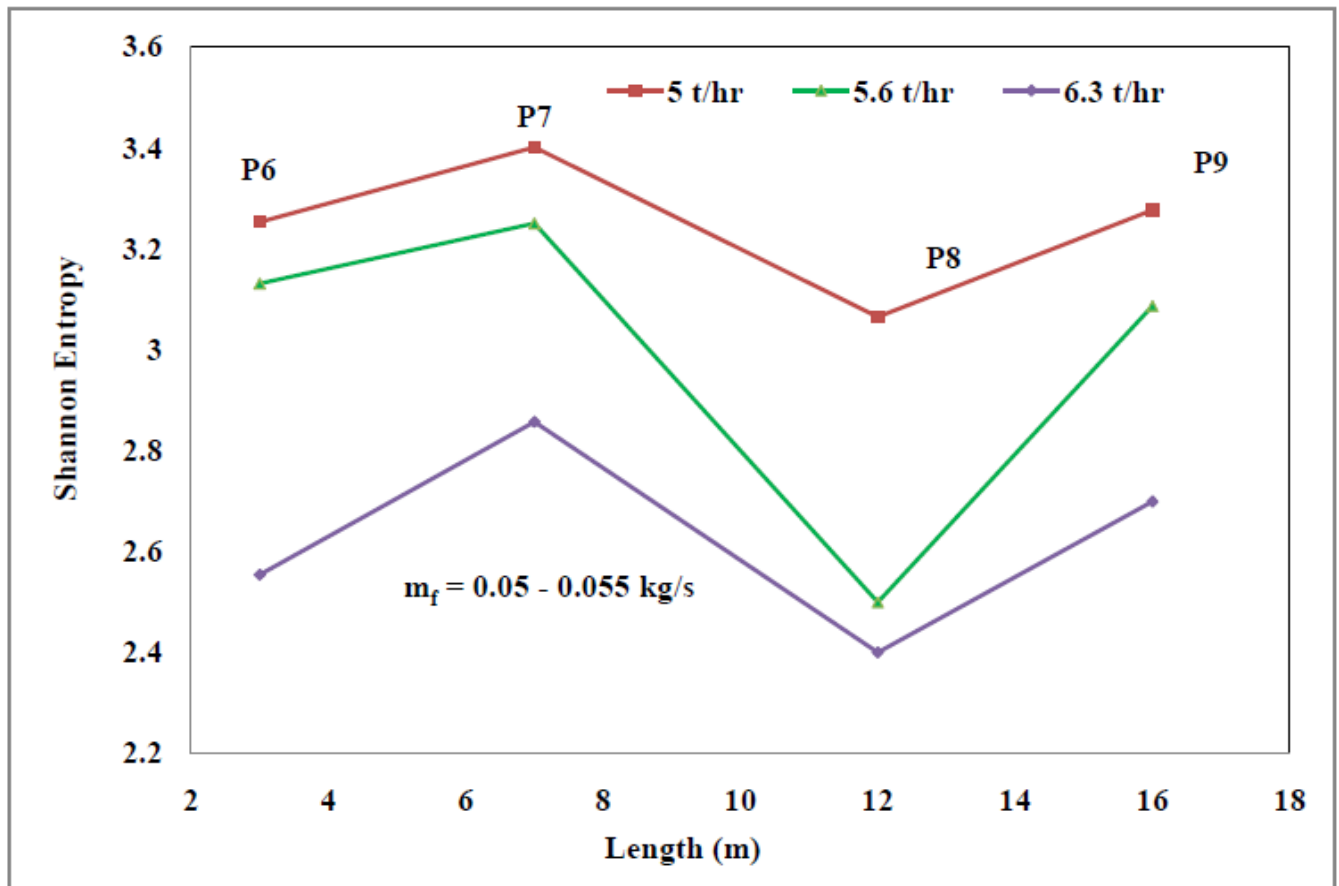


**Figure 5.13:** Shannon Entropy versus length for fly ash at varying  $m_s$

(63 mm I.D. x 24 long pipeline)

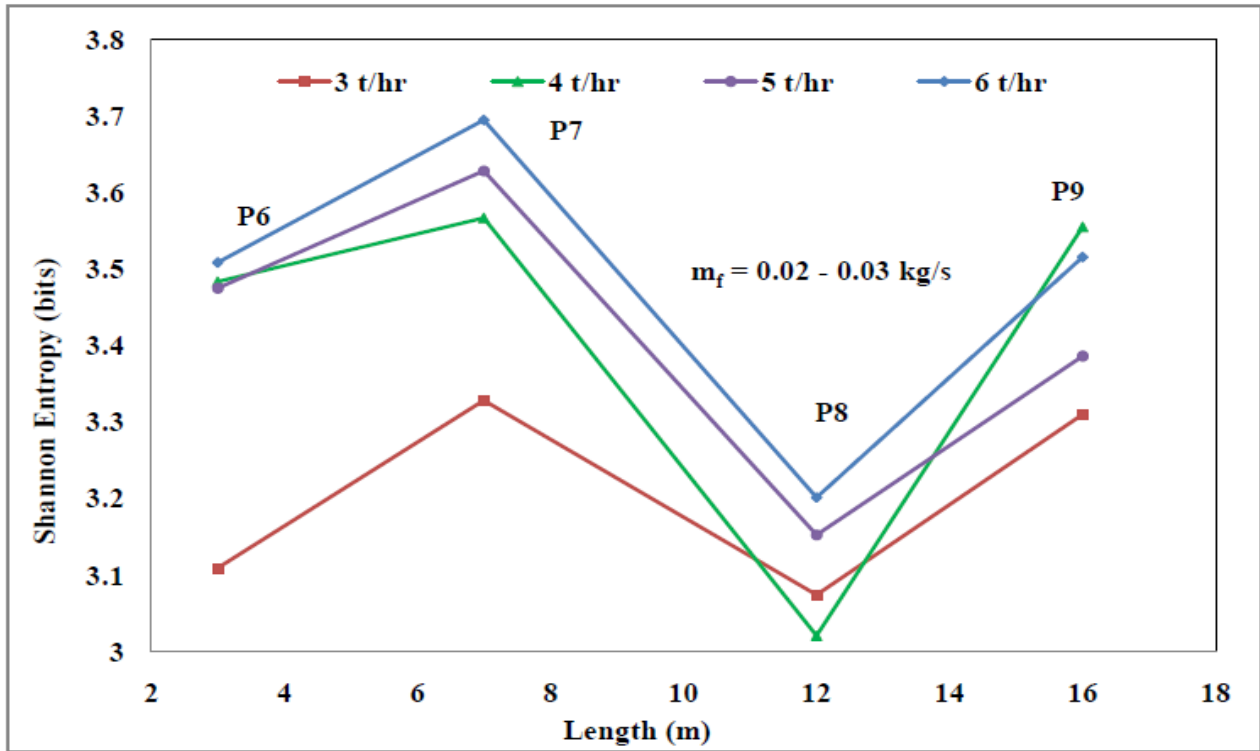


Figure 5.14: Shannon entropy versus length for fly ash at varying  $m_s$  (63 mm I.D. x 24 long pipeline)

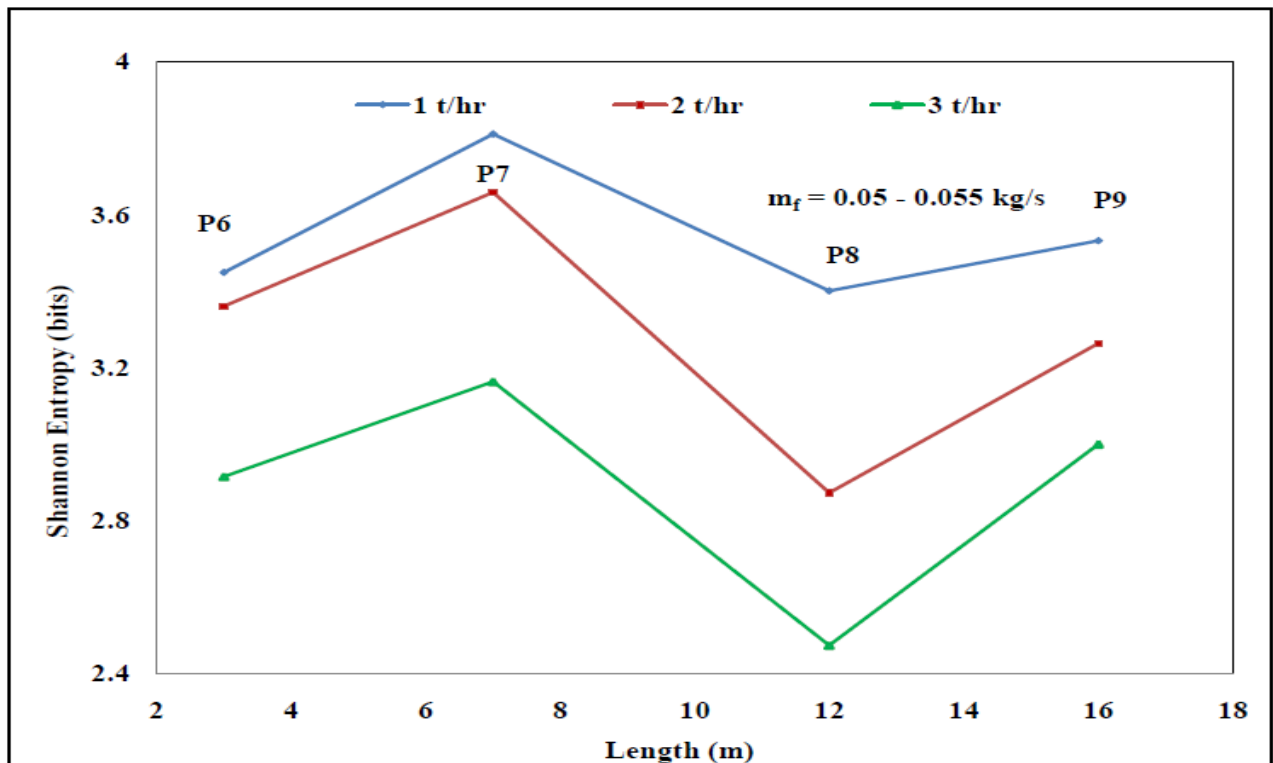
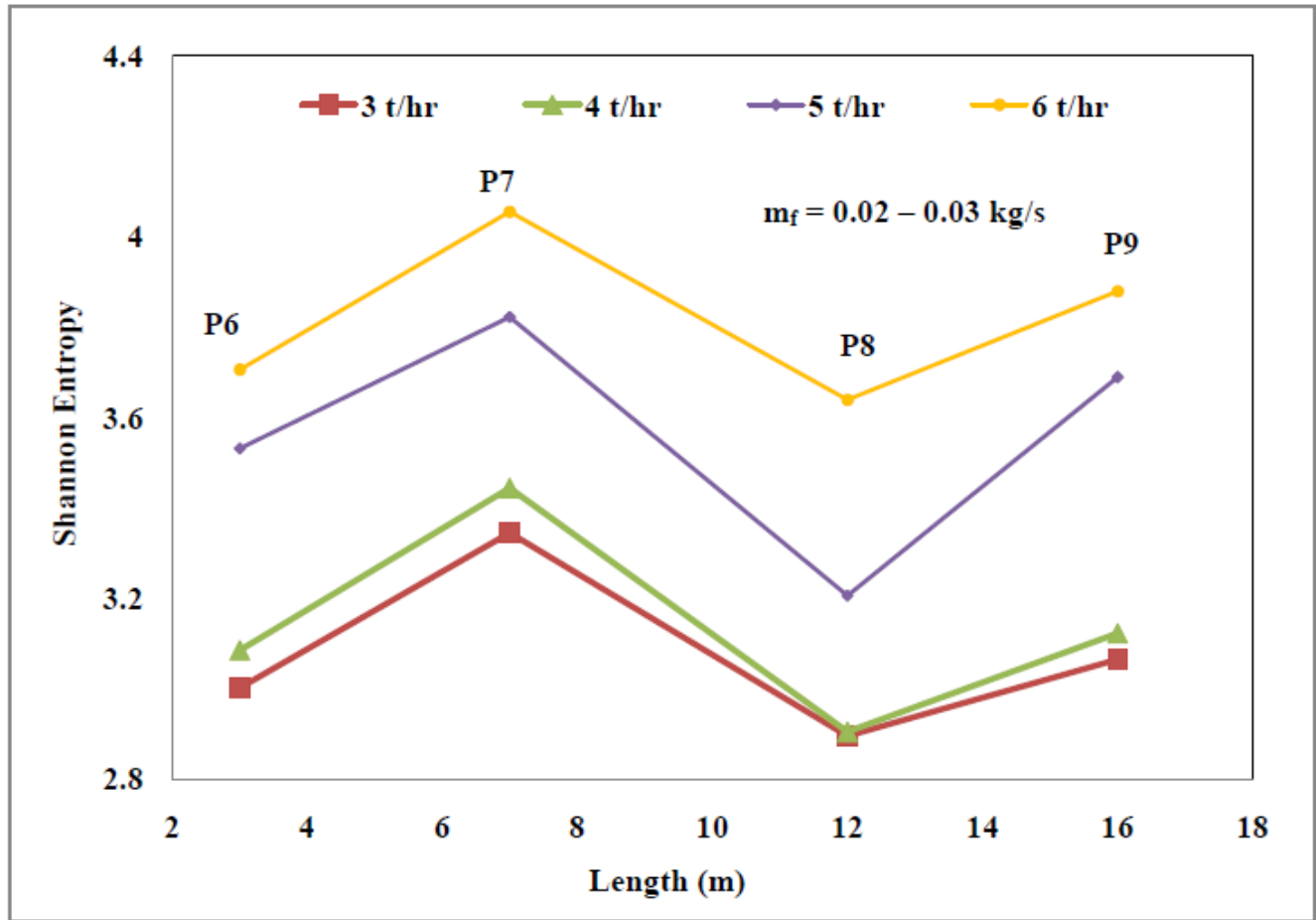


Figure 5.15: Shannon Entropy versus length for cement at varying  $m_s$  (63 mm I.D. x 24 long pipeline)



**Figure 5.16:** Shannon Entropy versus length for cement at varying  $m_s$   
(63 mm I.D. x 24 long pipeline)

It is observed that Shannon entropy value increases with increase in  $m_s$  at constant  $m_f$  (0.02 – 0.03 kg/s). Higher values of Shannon entropy for all pressure transducers (P6 to P9) is obtained for higher solid mass flow rate. However, Figure 5.15 shows decrease in value of Shannon entropy with increase in  $m_s$  at higher value of  $m_f$  (0.05 – 0.055 kg/s). Change in trend of Shannon entropy with increase in  $m_s$  for different values of  $m_f$  may be due to different solid loading ratio obtained in both cases. Solid loading ratio is defined as ratio of solid mass flow rate

( $m_s$ ) to air mass flow rate ( $m_f$ ). Higher solid loading ratio (above 40) is obtained in this study for range of  $m_f$  (0.02 – 0.03 kg/s) and lower value of solid loading ratio (below 20) for mentioned higher  $m_f$  (0.05 – 0.055 kg/s) at same value of  $m_s$ . Addition of material into higher gas flow rate tends to reduce the gas phase turbulence (Mittal, 2015), makes the flow smooth and reduces disorder of pressure fluctuations indicate by reducing value of Shannon entropy. While at higher solid loading ratio, addition of more solid particles tends to increase the pressure fluctuations which causes rise in Shannon entropy. Probable explanation is that due to presence of more solid, particle to particle collision (Dhodapkar, 1993) effect dominates over turbulence effect of gas. Feeding of more solid is apt to form the deposit near the bottom of pipe and lead the system towards unsteady state conditions. Similar variations can be seen in case of cement for both range of  $m_f$ . Higher range of Shannon entropy (3.7 to 4.0) is obtained for cement compared to fly ash (3.4 to 3.7) at same value of  $m_f$  and  $m_s$  with due to its different particle properties (small particle diameter and more particle density) shown by figure 5.16.

Figure 5.17 and 5.18 presents the changes in Shannon entropy value with respect to solid loading ratio for fly ash and cement, respectively. These graphs show the continuous variation in Shannon entropy for all pressure transducers (P6 to P9) with increase in value of solid loading ratio. It can be seen that at low solid loading ratio, Shannon entropy decreases with increase in solid loading ratio up to certain extent, reaches minimum value and then increases with further increase in solid loading ratio. It shows the same trend as shown by previous figures made in between of Shannon entropy and length of pipeline covering number of experiments instead of taking few experiments into consideration.

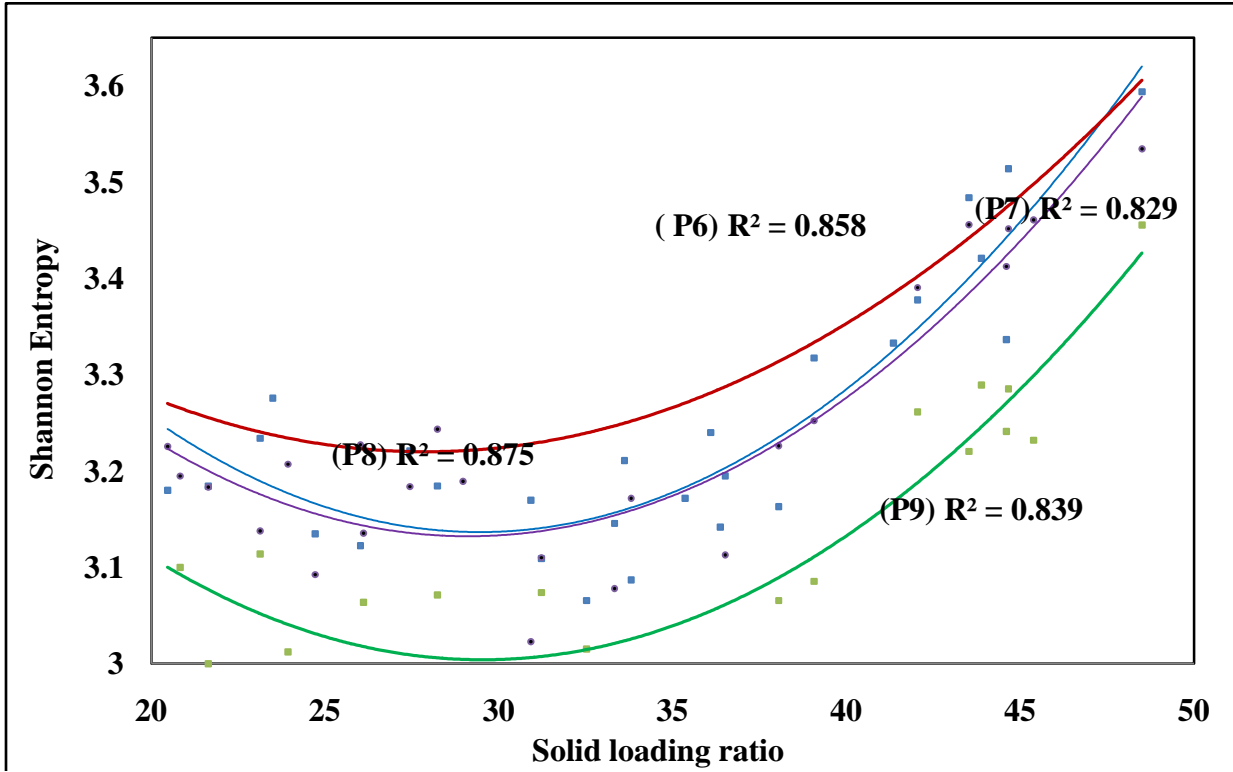


Figure 5.17: Shannon entropy versus solid loading ratio for fly ash (63.5 mm I.D. x 24 m long pipeline)

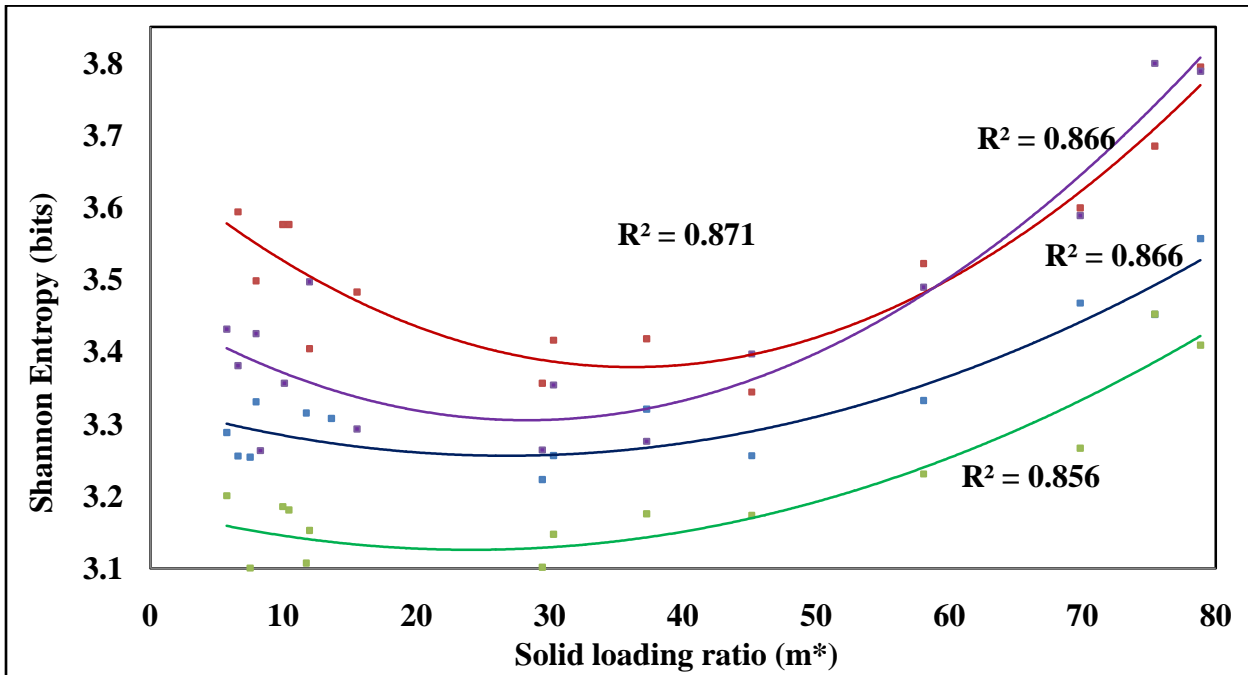


Figure 5.18: Shannon entropy versus solid loading ratio for cement (63.5 mm I.D. x 70 m long pipeline)

## **CHAPTER 6: CONCLUSION AND FUTURE SCOPE OF WORK**

\*

## 6.1 Conclusion

Lot of experiments has been done using cement and fly ash as conveying material through different pipeline to get different pressure fluctuations pattern in order to meet the objectives in this study. Based on the results of experimental work, following conclusions can be made:

- Shannon entropy value increases along straight sections of pipelines in flow direction due to increasing turbulence and complexity of flow along the straight sections. However, decreasing trend in value of Shannon entropy can be seen during flow after the bend. This could be due to suppressed pressure fluctuations as the particles are slow down during flow through bend (Mittal, 2014).
- Overall value of Shannon entropy remain same for smaller pipeline (63 mm I.D. x 24 m long) and decrease in overall value for longer pipeline (51 mm I.D. x 70 m long) for both products compared to overall increase in value in previous work (Mittal,2014). It may be due to the reason that experiments conducted in small length pipelines (24m and 70m) relative to large length pipelines (148m and 168m ) used in previous work and also due to two bends coupled with comparatively shorter length pipelines in this study.
- Higher range of Shannon entropy value and standard deviation is obtained in case of cement than fly ash for both pipelines due to different particle properties.
- Higher value of Shannon entropy is obtained for low velocities (2-5 m/s) for both products. Small conveying velocity in pipeline leads to deposition of particles at bottom of pipeline and further decrease in velocity can cause blockage in pipeline so sharp rise in Shannon entropy in low velocities region could be indication of forthcoming blockage.

- Increase in solid mass flow rate causes the increase in value of Shannon entropy at higher solid loading ratio but shows reverse trend for lower solid loading ratio.

From this investigation, it can be observed that variation of Shannon entropy value represents the effect of changes in conveying parameters and this support of Shannon entropy with these conveying parameters make it useful to identify the flow regime, variation in flow mechanism and flow characteristics.

## **6.2 Future scope of work**

During this study or investigation of pressure fluctuations, it has been observed, there is still much information into these transient pressure pulses which need to be extracted and lot of unknown factors need to be known. Some of these aspects for future work are suggested as follows:

- Effect of other components such as air feeder (compressor, blower) and material feeder (blow tank) which are also responsible for transient behavior of pressure pulses. Identification of signals generated by these components should be done.
- Effect of feed rate of solids into pipeline and effect of variation in types of supply air (top air, fluidizing air) on pressure fluctuations.
- Further investigation of pressure fluctuations using Shannon entropy or any other technique to know about power consumption by pneumatic conveying system.
- Try different signal processing techniques and analysis to investigate the pressure signals more accurately and precisely.

## **REFERENCES**

- Cho, Y.J., Kim, S.J., Nam, S.H. Kang, Y. and Kim. S.D. (2001). Heat transfer and bubble properties in three-phase circulating fluidized beds. *Chemical Engineering Science*, 56, 6107-6115.
- Dhodapakar, S. V. and Klinzing, G. E. (1993). Pressure fluctuations in pneumatic conveying. *Powder Technology*, 74(2), 179-195.
- Duan, F. and Cong, S. (2013). Shannon entropy analysis of dynamic behavior of Geldart group B and Geldart group D particles in a fluidized bed. *Chemical Engineering Communications*, 200(4), 575-586.
- Jaiboon, O., Chalermssinsuwan, B., Mekasut, L. and Piumsomboon, P. (2013). Effect of flow pattern on power spectral density of pressure fluctuation in various fluidization regimes. *Powder Technology*, 233, 215-226.
- Jama, G. A., Klinzing, G.E. and Rizk, F. (2000). An investigation of the prevailing flow pattern and pressure fluctuation near the pressure minimum and unstable conveying zone of pneumatic transport systems. *Powder Technology*, 112, 87-93.
- Klinzing, G.E., Rizk, F., Marcus, R. and Leung, L.S. Springer. Pneumatic conveying of solids. Third Edition. 2009.
- Li, H. (2002). Application of wavelet multi-resolution analysis to pressure fluctuations of gas solid two phase flow. *Powder Technology*, 125, 61-73.
- Liang, C., Zhao, C.S., Chen, X.P., Pu, W.H. and Fan C.L. (2007). Flow Characteristics and Shannon Entropy Analysis of Dense-Phase Pneumatic Conveying of Pulverized Coal with Variable Moisture Content at High Pressure. *Chemical Engineering Technology*, 30, 926-931.

- Liang, C., Liu, S., Pan, Xu., Guiling, Xu., Gaoyang, Y., Xiaoping, C. and Changsui, Z. 2014. Comparison of pressure drop through different bends in dense phase pneumatic conveying system at high pressure. *Powder Technology*. 57: 11-19.
- Mallick, S.S. (2010). PhD Dissertation: Modeling Dense-phase Pneumatic Conveying of Powders, University of Wollongong.
- Mallick, S.S and Wypych, P.W. (2009). Minimum transport boundaries for pneumatic conveying of powders. *Powder Technology*, 194, 181–186.
- Mittal, A., Mallick, S.S. and Wypych, P.W. (2014). An Investigation into flow mode transition and pressure fluctuations for fluidized dense phase pneumatic conveying of fine powders. *Particology*, 187-195
- Mittal, A., Mallick, S.S. and Wypych, P.W. (2015). An investigation into pressure fluctuations for fluidized dense-phase pneumatic transport of fine powders. *Powder Technology*, 277, 163-170.
- Ommen, J., Schaaf, J., Schouten, J., Wachem, B. and Bleek, C. 2004. Optical Placement of probes for dynamic pressure measurement in large scale fluidized bed. *Powder technology*. 139: 264-276.
- Pahk, J.B. (2006). PhD Dissertation: Experimental study of pressure fluctuation in pneumatic conveying by various methods of analysis, University of Pittsburgh.
- Pan, R. (1999). Material properties and flow modes in pneumatic conveying. *Powder Technology*, 104, 157-163.
- Pan, R. 1992. PhD Dissertation: Improving scale up procedures for the design of pneumatic conveying system, University of Wollongong.

- Plasynski, S.I., Klinzing, G.E. and Mathur, M.P. 1994. High pressure vertical pneumatic transport investigation. *Powder technology*. 79: 95-109
- Ratnayake, C. 2005. PhD Dissertation: A Comprehensive scaling up technique for pneumatic transport systems, Telemark University College (HiT-TF) Kjølnes Ring, N-3914 Porsgrunn, Norway
- Ren, J., Mao, O., Li, J., and Lin, W. 2001. "Wavelet analysis of dynamic behavior in fluidized beds. *Chemical engineering science*, 26: 981-988.
- Setia, G. 2012. Master of Engineering: Modelling Minimum Transport boundary for dense phase pneumatic conveying of fine powder. Thapar University. India
- Shannon, C.E. (1948). A mathematical theory of communication, *Bell System Technology*, 27, 379-423.
- Venkatasubramanian, S., Tashiro, H., Klinzing, G.E. and Mykelbust, K. (2000). Solid flow behavior in bends: assessing fine solids buildup. *Powder Technology*, 113, 124-131.
- Williams, K.C., Jones, M.G., and Cenna A.A. (2008). Characterization of the gas pulse frequency, amplitude and velocity in non-steady dense phase pneumatic conveying of powders. *Particology*, 6, 301-306.
- Wypych, P.W. (1989). PhD Dissertation: Pneumatic conveying of bulk solids, University of Wollongong.
- Wypych, P.W. 2006. Course Notes on Introduction to Pneumatic Conveying. University of Wollongong.

## Appendix A1

**TABLE A1.1: Shannon entropy values for fly ash (63 mm I.D. x 24 m long pipeline)**

Sr. No	Pressure Transducer Location	Shannon Entropy Values (bits) along the length			
		p6	p7	p8	p9
	Pipeline length (m)	3	7	13	16
	Name				
1	Exp1	3.045	3.0616	2.706	3.0131
2	Exp2	3.3446	3.4965	3.2905	3.4436
3	Exp3	2.6685	2.7215	2.3455	2.611
4	Exp4	3.5517	3.7004	3.0639	3.2355
5	Exp7	3.135	3.248	3.4831	3.0926
6	Exp8	3.1845	3.479	3.1982	3.2834
7	Exp9	3.2054	3.4114	2.9543	3.2588
8	Exp10	3.2341	3.4557	2.8114	3.28
9	Exp11	3.2759	3.5261	3.2954	2.8557
10	Exp12	3.2109	3.2637	3.4379	2.4974
11	Exp13	3.1302	3.2492	2.4981	3.0856
12	Exp14	2.9415	3.1508	2.6953	3.3754
13	Exp15	2.7501	3.0557	2.8096	3.1649
14	Exp16	2.8099	2.9602	2.5179	2.7826
15	Exp17	3.1226	3.2165	2.9295	3.2274
16	Exp19	2.9697	3.2128	2.6962	3.0229
17	Exp21	3.1632	3.3185	3.0656	3.4264
18	Exp23	3.7089	3.8956	2.9955	3.5161
19	Exp24	3.3367	3.5293	3.2412	3.4125
20	Exp22	3.6841	3.7525	3.055	3.5517
21	Exp27	3.121	3.3884	3.4895	2.78
22	Exp28	3.284	3.5672	3.0205	3.5558
23	Exp29	3.7339	3.6284	3.7256	3.7147
24	Exp31	3.3775	3.5714	2.9453	3.2524
25	Exp33	3.1092	3.2285	3.174	3.3102
26	Exp35	3.1457	3.6529	3.1445	3.578
27	Exp41	2.6406	3.0991	2.3242	2.6028
28	Exp47	2.7446	2.9564	2.531	2.8737
29	Exp52	3.0551	3.2871	2.9321	3.1908

**TABLE A1.2: Shannon entropy values for fly ash (51 mm I.D. x 70 m long pipeline)**

Sr. No	Pressure Transducer Location	Shannon Entropy values (bits) along the length			
		p6	p7	p8	p9
	Pipeline Length (m)	3	21	44	62
	Name				
1	Exp1	3.6236	3.7798	2.8014	3.236
2	Exp2	3.3258	3.4083	2.6041	3.0019
3	Exp3	2.3429	2.5999	2.1165	2.2784
4	Exp4	3.5773	3.6772	2.7053	3.0642
5	Exp5	3.0685	3.2204	2.4771	2.8504
6	Exp6	3.033	3.2581	2.0387	2.3066
7	Exp7	3.5242	3.5743	2.0232	2.8832
8	Exp8	3.0758	3.1918	2.2323	2.8543
9	Exp9	3.4585	3.5389	2.0645	2.3558
10	Exp10	3.5553	3.6963	3.1175	3.1475
11	Exp11	3.1017	3.1463	2.5622	3.1056
12	Exp12	2.513	2.5555	2.3291	2.4003
13	Exp14	3.1409	3.4562	2.9256	3.354
14	Exp15	3.2616	3.4333	2.7247	3.2771
15	Exp17	2.6678	2.9422	2.3006	2.4589
16	Exp18	3.4598	3.6801	2.4631	1.9444
17	Exp19	3.5195	3.8924	2.5746	2.7955
18	Exp21	2.6655	2.8749	2.7469	2.5382
19	Exp22	2.7454	2.8846	2.3579	2.7407
20	Exp23	2.2917	2.3724	2.0285	1.7018
21	Exp25	3.0577	3.1459	2.9102	3.0421
22	Exp26	2.2645	2.6893	2.7736	2.3511
23	Exp27	2.6972	2.9627	2.078	2.9708
24	Exp28	3.667	3.2653	2.3749	2.3749
25	Exp29	2.5425	2.6657	2.6772	2.2865
26	Exp32	2.6083	2.8149	2.3339	2.5296
27	Exp33	2.6852	2.8488	2.5874	2.7833
28	Exp34	2.3992	2.7583	2.4747	2.6093
29	Exp35	2.2462	2.724	2.5305	2.8089
30	Exp36	2.3645	2.5162	2.0577	2.3397

**TABLE A1.3: Shannon entropy values for cement (63 mm I.D. x 24 m long pipeline)**

Sr. No	Pressure Transducer Location	Shannon Entropy values (bits) along the length			
		p6	p7	p8	p9
	Pipeline Length (m)	3	7	13	16
	Name				
1	Exp1	3.8325	3.9346	3.7296	3.899
2	Exp2	3.4676	3.4994	3.6212	3.529
3	Exp3	3.8269	3.8948	3.8094	4.0753
4	Exp4	3.4563	3.5458	3.4774	3.5918
5	Exp5	2.6677	2.9848	2.3311	2.7603
6	Exp6	3.6062	3.757	3.374	3.6393
7	Exp7	3.6045	3.8786	3.2739	3.9095
8	Exp9	2.2064	2.4014	2.1313	2.3659
9	Exp10	2.9674	3.4162	3.1473	3.3541
10	Exp11	2.3304	2.5997	1.8104	2.3107
11	Exp12	3.1019	3.625	3.4523	3.8997
12	Exp14	1.907	2.1544	2.3531	2.7186
13	Exp17	3.1631	3.0026	3.0016	2.145
14	Exp19	3.7206	3.9181	3.3755	3.576
15	Exp20	3.732	3.9205	3.264	3.9862
16	Exp21	3.5542	3.7802	3.5952	3.747
17	Exp22	3.3309	3.4983	2.8551	3.2252
18	Exp23	3.6552	3.7938	3.4073	3.7478
19	Exp24	3.5078	3.6716	2.8526	3.4759
20	Exp25	3.3472	3.788	3.3686	3.593
21	Exp26	3.5324	3.6723	3.2307	3.4896
22	Exp27	2.8869	3.5765	3.1809	3.3607
23	Exp28	2.8869	3.5765	2.6436	2.8459
24	Exp29	3.1941	3.3234	3.1004	3.3277
25	Exp30	2.823	3.3044	2.9502	3.397
26	Exp31	2.7313	2.9524	2.9833	2.9191
27	Exp32	2.9147	3.163	2.4731	2.9992
28	Exp33	3.5604	3.7585	2.8724	3.2631
29	Exp34	3.2082	3.8104	3.4006	3.4313
30	Exp35	3.1556	3.594	2.7361	3.0509

**TABLE A1.4: Shannon entropy values for cement (51 mm I.D. x 70 m long pipeline)**

Sr. No	Pressure Transducer Location	Shannon Entropy Values (bits) along the length			
		p6	p7	p8	p9
	Pipeline Length (m)	3	21	44	62
1	Exp1	3.5257	3.8173	3.496	3.6456
2	Exp2	3.7514	3.9264	3.8271	2.9596
3	Exp3	3.7184	3.6784	3.9075	3.326
4	Exp4	4.0814	3.8522	3.9974	3.6106
5	Exp5	4.0267	4.1119	4.0941	3.2822
6	Exp6	4.0085	4.0873	4.0871	3.2606
7	Exp7	3.9602	3.8159	4.0125	3.4105
8	Exp8	3.5153	3.9664	3.1405	3.3452
9	Exp9	3.032	3.7163	3.127	3.254
10	Exp10	4.0191	4.1115	3.516	2.7522
11	Exp11	3.421	3.9261	3.313	3.4612
12	Exp12	3.1621	3.5391	2.8639	3.121
13	Exp13	4.0034	3.952	3.8874	3.5248
14	Exp14	4.0532	3.9632	4.0401	3.2582

## Appendix 2

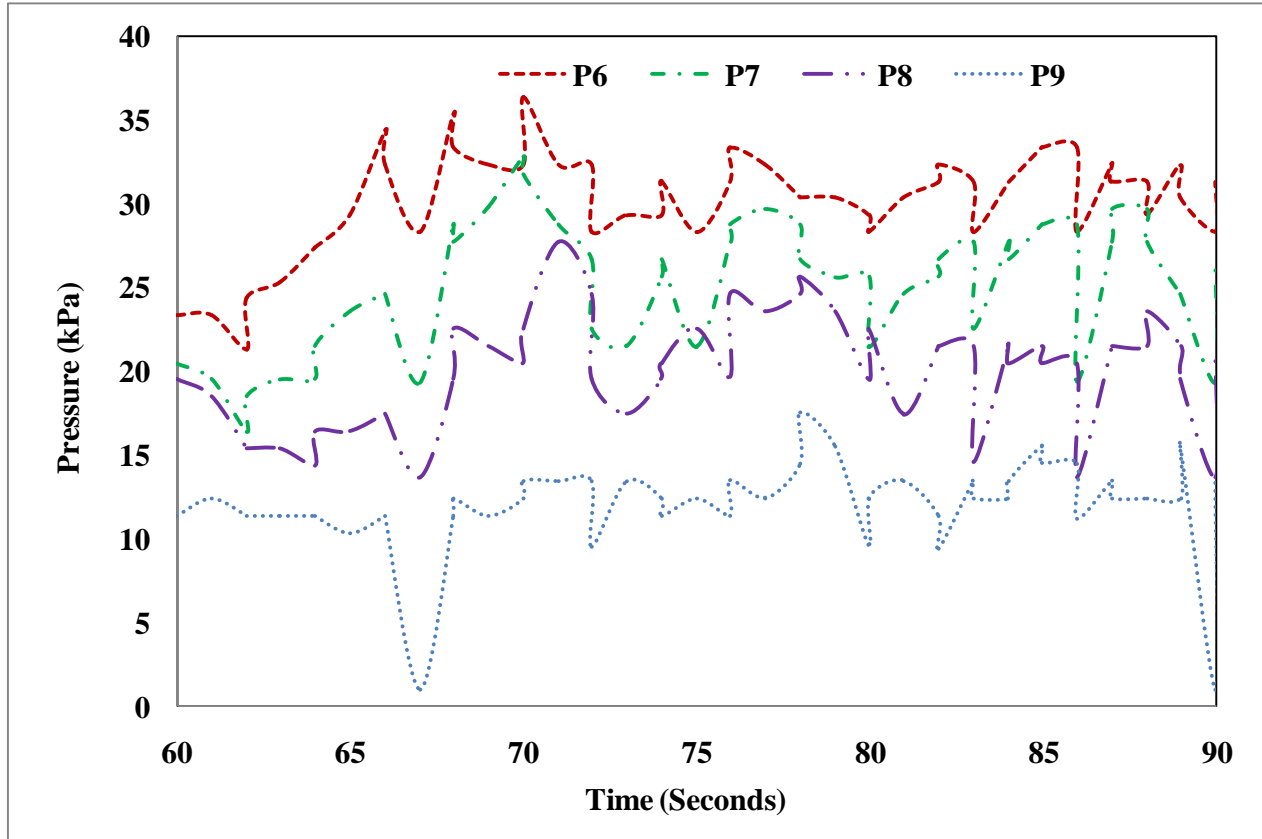


**Figure A2.1:** Pressure fluctuations (P6 to P9) for cement (63.5 mm I.D. x 24 m long pipeline)

( $m_f = 0.023$  kg/s,  $m_s = 2$  t/hr)

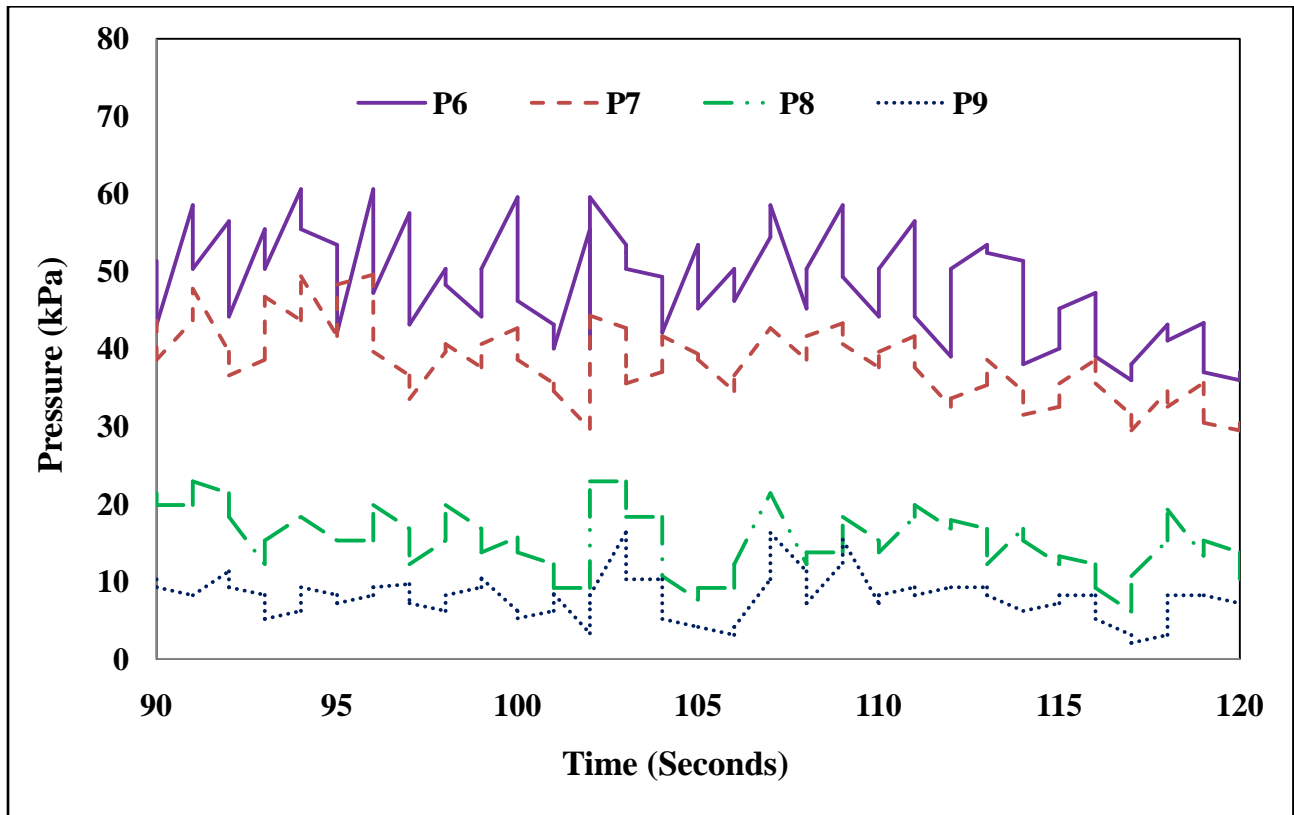


**Figure A2.2:** Pressure fluctuations (P6 to P9) for cement (51 mm I.D. x 70 m long pipeline)

( $m_f = 0.042$  kg/s,  $m_s = 2.4$  t/hr)

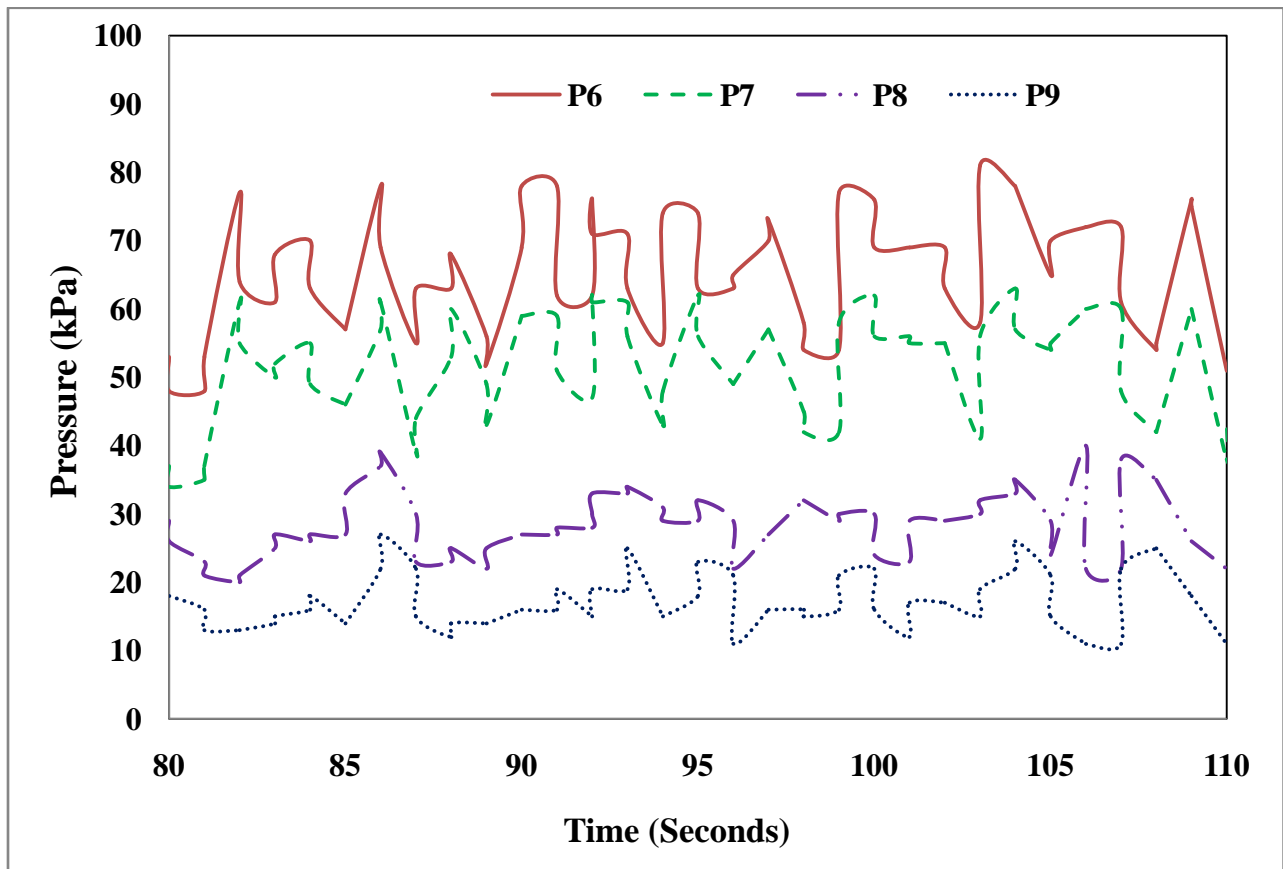


**Figure A2.3:** Pressure fluctuations (P6 to P9) for fly ash (51 mm I.D. x 24 m long pipeline)

( $m_f = 0.042$  kg/s,  $m_s = 4$  t/hr)

## **Communications**

**Goel, A.,** Mittal, A. and Mallick, S.S. An Experimental investigation into transient pressure pulses during pneumatic conveying of fine powders using Shannon entropy. **Chemical Engineering Communications, Taylor and Francis.**